ESAIM: M2AN 57 (2023) 2397–2426
https://doi.org/10.1051/m2an/2023038

ESAIM: Mathematical Modelling and Numerical Analysis
www.esaim-m2an.org

FULLY DISCRETE SCHWARZ WAVEFORM RELAXATION ANALYSIS FOR THE HEAT EQUATION ON A FINITE SPATIAL DOMAIN

Ronald D. Haynes* and Khaled Mohammad

Abstract. Schwarz waveform relaxation methods provide space-time parallelism for the solution of time dependent partial differential equations. The algorithms are differentiated by the choice of the transmission conditions enforced at the introduced space-time boundaries. Early results considered the theoretical analysis of these algorithms in the continuous and semi-discrete (in space) settings for various families of linear partial differential equations. Later, fully discrete results were obtained under the simplifying assumption of an infinite spatial domain. In this paper, we provide a first analysis of a fully discrete classical Schwarz Waveform algorithm for the one-dimensional heat equation on an arbitrary but finite number of bounded subdomains. The θ-method is chosen as the time integrator. Convergence results are given in both the infinity norm and two norm, with an explicit contraction given in the case of a uniform partitioning. The results are compared to the numerics and to the earlier theoretical results.

Mathematics Subject Classification. 65M55, 65M12, 65M15, 65Y05, 35K05.

Received May 11, 2022. Accepted April 28, 2023.

1. Introduction

Schwarz waveform relaxation (SWR) provides space–time parallelism by partitioning the computational domain into overlapping or non-overlapping subdomains and iteratively solving the time dependent partial differential equations (PDEs) over a time window. The convergence characteristics depend on the family of PDE, the choice of spatial and temporal discretization, and the transmission conditions which couple the subdomain problems together at the subdomain boundaries. The use of Dirichlet transmission conditions at the (often) artificial interior interfaces defines a classical SWR algorithm. The iteration may be improved tremendously by enforcing continuity of higher order operators at these interfaces, giving rise to a family of optimized SWR algorithms.

The analysis of classical SWR at the continuous, semi-discrete, and fully discrete levels has been provided for many classes of PDEs. The first results by Gander and Stuart [9] analyzed SWR for the heat equation in continuous and semi-discrete settings on a finite spatial domain. Giladi and Keller [16] analyzed the continuous classical SWR method for the advection diffusion equation in one and two spatial dimensions. The analyses show linear convergence on unbounded time intervals and superlinear convergence on bounded time intervals. The contraction rates depend on the coefficients of the PDE, the size of the overlap and time window, and

Keywords and phrases. Heat equation, Domain decomposition, Schwarz waveform relaxation.

Department of Mathematics & Statistics, Memorial University of Newfoundland, St. John's, Newfoundland A1C 5S7, Canada.
*Corresponding author: rhaynes@mun.ca

the number of subdomains. Similar results have been obtained for nonlinear reaction-diffusion equations in one spatial dimension in [7], for convection-dominated nonlinear conservation laws in [11], and convergence in a finite number of steps was obtained for the wave equation in [12]. The slow convergence of classical SWR can be improved greatly by replacing the Dirichlet transmission conditions at the interior interfaces by local approximations to the Dirichlet to Neumann operators for each subdomain. This leads to a family of optimized Schwarz algorithms, see [8] in the steady case, [3, 4, 13] for advection-reaction-diffusion problems, and [12, 14] for the wave equation. For some classes of problems, classical SWR can be accelerated using improved initial guesses generated by a multirate approach [19].

The early semi-discrete (in space) analysis for the heat equation in [9] was extended in [24] to give a semi-discrete (in space) analysis for classical and optimized SWR for reaction diffusion equations on an infinite spatial domain. In [1, 2, 10, 15] continuous in time analysis was provided for closely related applications to RC type circuits. Discrete in time analysis for an infinite circuit may be found in [26], while [25, 27] provides results for a fractional order, infinite circuit, in both the discrete and continuous settings in time. Fully discrete analysis for Schrödinger's equation and the wave equation can be found in [17] and [14] respectively. In a very recent paper, Clement *et al.* [6] provide a fully discrete analysis for the reaction–diffusion problems on two unbounded spatial domains.

The fully discrete analyses mentioned above, all assume an infinite spatial domain to simplify the analysis. The boundedness of the error at $\pm\infty$ leads to a simpler solution of the error recursion. Furthermore, the contraction rate for the error becomes much easier to analyze. In this paper, we discuss the fully discrete convergence analysis of the SWR-algorithm for the heat equation on a bounded spatial domain using standard finite differences in space and the θ-method ($1/2 \leq \theta \leq 1$) in time. The consideration of a bounded spatial domain allows a multi-domain convergence analysis on a finite number of bounded domains while a bounded time domain reflects the usual practice of exchanging information between neighboring subdomains after a time window $[0, T]$. The bounded space and time domains also reflect the situation most often faced in actual computation. Many of the discrete analyses above only prove convergence at the interior interfaces only. Here we complete the picture by proving and utilizing a discrete maximum principle.

We show that the contraction rate for the fully discrete algorithm is bounded by the contraction rate for the semi-discrete and continuous cases on an unbounded time interval. On a bounded time interval, $[0, T]$, we prove that the contraction rate is bounded by the contraction rate of the algorithm on an unbounded time interval.

We mention that a brief sketch of a fully discrete analysis on two overlapping, bounded subdomains using backward Euler as the time integrator can be found in [18]. That special case analysis used a different proof technique.

Our model problem is the one dimensional heat equation $u_t = u_{xx} + f(x,t)$ for $-L < x < L$ and $t > 0$ subject to initial and boundary conditions $u(x,0) = u_0(x)$, $u(-L,t) = h_1(t)$, and $u(L,t) = h_2(t)$. To ensure a unique solution, we assume that f is bounded on $[-L, L] \times [0, \infty)$ and uniformly Hölder continuous on each compact subset of the space-time domain, and $u_0(x), h_1(t)$ and $h_2(t)$ are (at least) piecewise continuous [5]. Although seemingly quite restrictive, the one-dimensional heat equation is the standard prototypical model parabolic problem. As mentioned previously, the emphasis and novelty here is a first analysis of a fully discrete SWR algorithm on a bounded spatial domain. As we will see the imposition of a bounded spatial domain increases the complexity of the analysis significantly. Following the pattern of existing continuous SWR analyses, extensions to higher dimensions and more general parabolic problems will follow.

We obtain our semi-discrete problem by discretizing in space with centred finite differences on $\Omega^h = \{x_m : x_m = -L + \Delta x(m+N), m = -N, \ldots, N\}$, where $\Delta x = \frac{L}{N}$. This leads to the system of IVPs

$$\frac{\mathrm{d}\mathbf{u}(t)}{\mathrm{d}t} = A\mathbf{u}(t) + \mathbf{f}(t), \ t > 0, \quad \mathbf{u}(0) = \mathbf{u}_0, \tag{1.1}$$

where $\mathbf{u}(t) \in \mathbb{R}^{2N-1}$ is the solution vector on the interior of Ω^h with components $u_m(t)$ which are the (semi-discrete) approximations of $u(x,t)$ at $x = x_m$ for $m = -(N-1), \ldots, (N-1)$. Here $A = \frac{1}{\Delta x^2}\mathrm{tridiag}(1, -2, 1) \in \mathbb{R}^{(2N-1)\times(2N-1)}$, where $\mathrm{tridiag}(a, b, c)$ is a tridiagonal matrix with constants a, b, and c on the sub-diagonal,

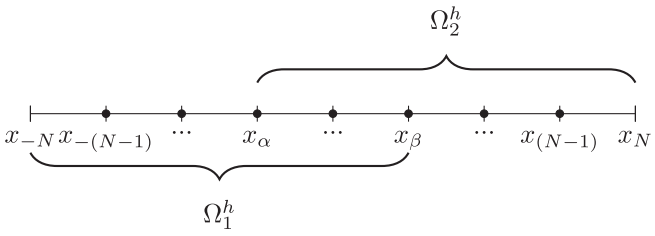

FIGURE 1. The spatial discrete decomposition.

main-diagonal, and super-diagonal, respectively. The inhomogeneity, $\mathbf{f}$, is given by

$$\mathbf{f}(t) = \left(f\big(x_{-(N-1)}, t\big) + \frac{1}{\Delta x^2} h_1(t), f\big(x_{-(N-2)}, t\big), \ldots, f\big(x_{(N-2)}, t\big), f\big(x_{(N-1)}, t\big) + \frac{1}{\Delta x^2} h_2(t) \right)^T,$$

and the initial vector $\mathbf{u}_0$ is given by $\mathbf{u}_0 = (u_0(x_{-(N-1)}), \ldots, u_0(x_{(N-1)}))^T$.

2. Convergence on two subdomains

We begin by decomposing Ω^h into two overlapping (discrete) subdomains: $\Omega_1^h = \{x_{-N}, x_{-(N-1)}, \ldots, x_\beta\}$ and $\Omega_2^h = \{x_\alpha, x_{\alpha+1}, \ldots, x_N\}$ where α and β are integers satisfying $-N < \alpha < \beta < N$, as shown in Figure 1.

The classical semi-discrete SWR algorithm for the heat equation on the two subdomains, Ω_1^h and Ω_2^h , can be written as: for $k = 1, 2, \ldots$, and for $j = 1, 2$ solve

$$\frac{\mathrm{d}\mathbf{u}_j^k(t)}{\mathrm{d}t} = A_j \mathbf{u}_j^k(t) + \mathbf{f}_j^k(t), \qquad t > 0, \tag{2.1a}$$

where

$$\mathbf{u}_1^k(t) = \left(u_{1,-(N-1)}^k(t), u_{1,-(N-2)}^k(t), \ldots, u_{1,(\beta-1)}^k(t) \right)^T, \tag{2.1b}$$

and

$$\mathbf{u}_2^k(t) = \left(u_{2,(\alpha+1)}^k(t), u_{2,(\alpha+2)}^k(t), \ldots, u_{2,(N-1)}^k(t) \right)^T, \tag{2.1c}$$

are the subdomain iterates on the interior nodes of Ω_1^h and Ω_2^h. Here, for $j = 1, 2$, $A_j = \frac{1}{\Delta x^2}\mathrm{tridiag}(1, -2, 1)$, where $A_1 \in \mathbb{R}^{(N+\beta-1)\times(N+\beta-1)}$ and $A_2 \in \mathbb{R}^{(N-\alpha-1)\times(N-\alpha-1)}$.

The vectors $\mathbf{f}_1^k \in \mathbb{R}^{N+\beta-1}$ and $\mathbf{f}_2^k \in \mathbb{R}^{N-\alpha-1}$, are defined by

$$\mathbf{f}_1^k(t) = \bar{\mathbf{f}}_1(t) + \frac{1}{\Delta x^2} u_{1,\beta}^k(t) \boldsymbol{\delta}_1 \quad \text{and} \quad \mathbf{f}_2^k(t) = \bar{\mathbf{f}}_2(t) + \frac{1}{\Delta x^2} u_{2,\alpha}^k(t) \boldsymbol{\delta}_2, \tag{2.1d}$$

where $\boldsymbol{\delta}_1 \in \mathbb{R}^{N+\beta-1}$ and $\boldsymbol{\delta}_2 \in \mathbb{R}^{N-\alpha-1}$, are the unit column vectors

$$\boldsymbol{\delta}_1 = (0, \ldots, 0, 1)^T \quad \text{and} \quad \boldsymbol{\delta}_2 = (1, 0, \ldots, 0)^T. \tag{2.1e}$$

The overbar notation, $\bar{\mathbf{f}}_j$, for $j = 1, 2$, denotes the first $N + \beta - 1$ and the last $N - \alpha - 1$ components of $\mathbf{f}$, respectively. This bar notation will be used in this manner throughout this section. The system (2.1a) is supplemented with an initial condition

$$\mathbf{u}_j^k(0) = \bar{\mathbf{u}}_j(0), \quad j = 1, 2, \tag{2.1f}$$

and boundary and Dirichlet transmission conditions

$$\begin{aligned} u^k_{1,-N}(t) &= h_1(t), & u^k_{1,\beta}(t) &= u^{k-1}_{2,\beta}(t), \quad t>0,\\ u^k_{2,\alpha}(t) &= u^{k-1}_{1,\alpha}(t), & u^k_{2,N}(t) &= h_2(t), \quad t>0. \end{aligned} \tag{2.1g}$$

Here $u^k_{j,m}(t)$ represents the numerical approximation of $u(x,t)$ at $x=x_m$ on Ω^h_j at the k^{th} iteration of the SWR algorithm. To get the iteration started we must pick initial guesses for $u^0_{2,\beta}(t)$ and $u^0_{1,\alpha}(t)$.

To analyze the fully discrete SWR we begin with a lemma which describes the single domain discrete solution of (1.1) using the θ-method.

Lemma 2.1. *The single domain solution at $t=t_n$, $\mathbf{u}(n)$, restricted to the interior of Ω^h_j, denoted $\bar{\mathbf{u}}_j(n)$, for $j=1,2$, using the θ-method to integrate the semi-discrete heat equation (1.1), are the unique solutions of the subsystems*

$$\begin{aligned} (I_1-\theta\Delta tA_1)\bar{\mathbf{u}}_\mathbf{1}(n)-\theta\Delta t\mathbf{f}_\mathbf{1}(n) &= (I_1-(\theta-1)\Delta tA_1)\bar{\mathbf{u}}_\mathbf{1}(n-1)-(\theta-1)\Delta t\mathbf{f}_\mathbf{1}(n-1),\\ (I_2-\theta\Delta tA_2)\bar{\mathbf{u}}_\mathbf{2}(n)-\theta\Delta t\mathbf{f}_\mathbf{2}(n) &= (I_2-(\theta-1)\Delta tA_2)\bar{\mathbf{u}}_\mathbf{2}(n-1)-(\theta-1)\Delta t\mathbf{f}_\mathbf{2}(n-1), \end{aligned}$$

where

$$\mathbf{f}_1(n)=\bar{\mathbf{f}}_1(n)+\frac{1}{\Delta x^2}u_\beta(n)\boldsymbol{\delta}_1 \quad \textit{and} \quad \mathbf{f}_2(n)=\bar{\mathbf{f}}_2(n)+\frac{1}{\Delta x^2}u_\alpha(n)\boldsymbol{\delta}_2, \tag{2.2}$$

for $n=1,2,\ldots$. Here, $\boldsymbol{\delta}_{1,2}$, are defined in (2.1e), $u_\beta(n)$ and $u_\alpha(n)$ are the single domain solutions at the interior interface nodes at time t_n, and $I_{1,2}$ are the $(N+\beta-1)\times(N+\beta-1)$ and $(N-\alpha-1)\times(N-\alpha-1)$ identity matrices, respectively. We set $\bar{\mathbf{f}}_j(n)\equiv\bar{\mathbf{f}}_j(t_n)$ for $j=1,2$.

Similar expressions for the SWR approximations are given in the next lemma.

Lemma 2.2. *The solution of (2.1a)–(2.1g) using the θ-method at $t=t_n$, $\mathbf{u}^k_j(n)$, for $j=1,2$, are the unique solutions of the subsystems*

$$\begin{aligned} (I_1-\theta\Delta tA_1)\mathbf{u}^\mathbf{k}_\mathbf{1}(n)-\theta\Delta t\mathbf{f}^\mathbf{k}_\mathbf{1}(n) &= (I_1-(\theta-1)\Delta tA_1)\mathbf{u}^\mathbf{k}_\mathbf{1}(n-1)-(\theta-1)\Delta t\mathbf{f}^\mathbf{k}_\mathbf{1}(n-1),\\ (I_2-\theta\Delta tA_2)\mathbf{u}^\mathbf{k}_\mathbf{2}(n)-\theta\Delta t\mathbf{f}^\mathbf{k}_\mathbf{2}(n) &= (I_2-(\theta-1)\Delta tA_2)\mathbf{u}^\mathbf{k}_\mathbf{2}(n-1)-(\theta-1)\Delta t\mathbf{f}^\mathbf{k}_\mathbf{2}(n-1), \end{aligned} \tag{2.3}$$

for $n=1,2,\ldots$. Here $\mathbf{f}^k_j(n)\equiv\mathbf{f}^k_j(t_n)$, for $j=1,2$, where the vectors $\mathbf{f}^\mathbf{k}_\mathbf{j}(t)$ are defined in (2.1d).

We denote the error between the single domain and SWR solutions on subdomain j at time step n, by $\mathbf{e}^k_j(n)=\mathbf{u}^k_j(n)-\bar{\mathbf{u}}_j(n)$ for $j=1,2$. Simply subtracting the representations of the single domain and SWR solutions from the previous two lemmas gives the following result.

Lemma 2.3. *For $j=1,2$, $k=1,2,\ldots$ and $n=1,2,\ldots$ the errors, $\mathbf{e}^k_j(n)$, satisfy*

$$\begin{aligned} (I_1-\theta\Delta tA_1)\mathbf{e}^\mathbf{k}_\mathbf{1}(n)-\mu\theta e^k_{1,\beta}(n)\boldsymbol{\delta}_1 &= (I_1-(\theta-1)\Delta tA_1)\mathbf{e}^\mathbf{k}_\mathbf{1}(n-1)-\mu(\theta-1)e^k_{1,\beta}(n-1)\boldsymbol{\delta}_1,\\ (I_2-\theta\Delta tA_2)\mathbf{e}^\mathbf{k}_\mathbf{2}(n)-\mu\theta e^k_{2,\alpha}(n)\boldsymbol{\delta}_2 &= (I_2-(\theta-1)\Delta tA_2)\mathbf{e}^\mathbf{k}_\mathbf{2}(n-1)-\mu(\theta-1)e^k_{2,\alpha}(n-1)\boldsymbol{\delta}_2, \end{aligned}$$

with initial condition

$$\mathbf{e}^k_j(0)=\bar{\mathbf{0}}_j, \quad \text{for } j=1,2,$$

and boundary conditions

$$\begin{aligned} e^k_{1,\beta}(n) &= e^{k-1}_{2,\beta}(n), & e^k_{1,-N}(n) &= 0,\\ e^k_{2,\alpha}(n) &= e^{k-1}_{1,\alpha}(n), & e^k_{2,N}(n) &= 0. \end{aligned} \tag{2.4}$$

Here, $\mu=\Delta t/\Delta x^2$ and $\bar{\mathbf{0}}_j$ for $j=1,2$ are appropriately sized zero vectors.

Using the boundary values and the definition of $A_{1,2}$ and $\boldsymbol{\delta}_{1,2}$ we directly obtain the following recursions for the errors.

Lemma 2.4. *Component-wise, for $j = 1, 2$, $k = 1, 2, \ldots$ and $n = 1, 2, \ldots$, the errors $\mathbf{e}^k_{j,m}(n)$ satisfy*

$$\begin{aligned}-\mu\theta e^k_{1,m-1}(n) + (1+2\mu\theta)e^k_{1,m}(n) - \mu\theta e^k_{1,m+1}(n)\\ = -\mu(\theta-1)e^k_{1,m-1}(n-1) + (1+2\mu(\theta-1))e^k_{1,m}(n-1) - \mu(\theta-1)e^k_{1,m+1}(n-1),\end{aligned}$$

for $m = -(N-1), \ldots, \beta - 1$, and

$$\begin{aligned}-\mu\theta e^k_{2,m-1}(n) + (1+2\mu\theta)e^k_{2,m}(n) - \mu\theta e^k_{2,m+1}(n)\\ = -\mu(\theta-1)e^k_{2,m-1}(n-1) + (1+2\mu(\theta-1))e^k_{2,m}(n-1) - \mu(\theta-1)e^k_{2,m+1}(n-1),\end{aligned}$$

for $m = \alpha + 1, \ldots, N - 1$.

To analyze these recursions for the error we use the discrete Laplace transform [23]. The discrete Laplace transform for a general vector $\mathbf{w} = (w(0), w(1), \ldots)^T$, defined on a regular (time) grids with step size Δt, is

$$\widehat{\mathbf{w}}(s) = \frac{\Delta t}{\sqrt{2\pi}} \sum_{n=0}^{\infty} z^{-n} w(n), \tag{2.5}$$

where $z = e^{s\Delta t}$, $s \in R_s$ where $R_s = \{s \,|s = \sigma + i\omega,\, \sigma > 0 \text{ and } |\omega| \le \pi/\Delta t\}$.

The recursions for the discrete Laplace transforms of the errors are recorded in the next lemma.

Lemma 2.5. *For $j = 1, 2$, $k = 1, 2, \ldots$ and $n = 1, 2, \ldots$, the discrete Laplace transforms of errors, $\widehat{\mathbf{e}}^k_{j,m}(s)$, satisfy*

$$\mu\widehat{e}^k_{1,m-1}(s) - (2\mu+\eta)\widehat{e}^k_{1,m}(s) + \mu\widehat{e}^k_{1,m+1}(s) = 0, \quad m = -(N-1), \ldots, (\beta-1),$$

and

$$\mu\widehat{e}^k_{2,m-1}(s) - (2\mu+\eta)\widehat{e}^k_{2,m}(s) + \mu\widehat{e}^k_{2,m+1}(s) = 0, \quad m = \alpha+1, \ldots, (N-1),$$

where the quantities μ, η, and z are given by $\mu = \frac{\Delta t}{\Delta x^2}$, $\eta = \frac{z-1}{\theta(z-1)+1}$ and $z = e^{s\Delta t}$, for $s \in R_s$.

Taking the Laplace transform of the boundary conditions gives

$$\begin{aligned}\widehat{e}^k_{1,\beta}(s) &= \widehat{e}^{k-1}_{2,\beta}(s), \qquad & \widehat{e}^k_{1,-N}(s) &= 0,\\ \widehat{e}^k_{2,\alpha}(s) &= \widehat{e}^{k-1}_{1,\alpha}(s), & \widehat{e}^k_{2,N}(s) &= 0.\end{aligned} \tag{2.6}$$

The solutions of these recursion relations are given in the next two lemmas.

Lemma 2.6. *The general solutions of the recursions for the Laplace transforms of the errors are given by*

$$\widehat{e}^k_{j,m}(s) = a^k_j \lambda_+^m + b^k_j \lambda_+^{-m}, \tag{2.7}$$

where $m = -N, \ldots, \beta$, if $j = 1$, and $m = \alpha, \ldots, N$, if $j = 2$, where λ_+ solves $\lambda^2 - \left(2 + \frac{\eta}{\mu}\right)\lambda + 1 = 0$ and is given explicitly by

$$\lambda_+ = 1 + \frac{\eta}{2\mu} + \frac{\sqrt{\eta^2 + 4\mu\eta}}{2\mu}, \tag{2.8}$$

where $\mu = \frac{\Delta t}{\Delta x^2}$, $\eta = \frac{z-1}{\theta(z-1)+1}$ and $z = e^{s\Delta t}, s \in R_s$. In the expression for λ_+, we have chosen the square root with positive real part.

The image of the analytic complex function, $\lambda_+(s), s \in R_s$, is bounded for $\theta \in (1/2, 1]$ and unbounded for $\theta = 1/2$, see Figure 2.

The coefficients $\left(a^k_j, b^k_j\right)^T =: \mathbf{c}^k_j$ in (2.7) are shown to satisfy a simple fixed point iteration in the next lemma.

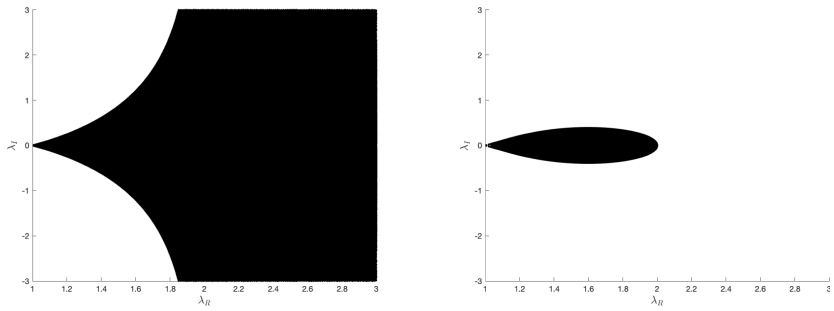

(a) (b)

FIGURE 2. The image of $\lambda_+(s), s \in R_s$ for $\theta = 1/2$ (*left*) and for $\theta = 1$ (*right*). (a) $\theta = 1/2$ and (b) $\theta = 1$.

Lemma 2.7. *The coefficients,* $\mathbf{c}_j^k = (a_j^k, b_j^k)^T$, *for* $j = 1, 2$, *in the general solution,* (2.7), *for the Laplace transforms of the errors satisfy*

$$\mathbf{c_1^k} = \Lambda_1^{-1}\Theta_1\mathbf{c_2^{k-1}} \quad \text{and} \quad \mathbf{c_2^k} = \Lambda_2^{-1}\Theta_2\mathbf{c_1^{k-1}}, \tag{2.9}$$

where

$$\Lambda_1 = \begin{pmatrix} \lambda_+^{-N} & \lambda_+^{N} \\ \lambda_+^{\beta} & \lambda_+^{-\beta} \end{pmatrix}, \ \Lambda_2 = \begin{pmatrix} \lambda_+^{\alpha} & \lambda_+^{-\alpha} \\ \lambda_+^{N} & \lambda_+^{-N} \end{pmatrix}, \ \Theta_1 = \begin{pmatrix} 0 & 0 \\ \lambda_+^{\beta} & \lambda_+^{-\beta} \end{pmatrix}, \quad \text{and} \quad \Theta_2 = \begin{pmatrix} \lambda_+^{\alpha} & \lambda_+^{-\alpha} \\ 0 & 0 \end{pmatrix}. \tag{2.10}$$

Proof. Using the error function in (2.7), the boundary conditions (2.4) can be written as

$$\Lambda_1\mathbf{c_1^k} = \Theta_1\mathbf{c_2^{k-1}} \quad \text{and} \quad \Lambda_2\mathbf{c_2^k} = \Theta_2\mathbf{c_1^{k-1}},$$

from which the result follows. □

To show convergence of the discrete SWR algorithm we show that $\widehat{e}_{1,m}^k(s)$ tends to zero as k tends to infinity for all relevant m. A straightforward, but slightly tedious calculation, gives the following recursions for the error functions $\widehat{e}_{1,\alpha}^k(s)$ and $\widehat{e}_{2,\beta}^k$.

Lemma 2.8. *If* $\lambda_+ = e^v$, *then the Laplace transforms of the errors in the approximation generated by the discrete SWR iteration* (2.3) *at the interfaces* x_α *and* x_β *satisfy*

$$\begin{aligned} \widehat{e}_{1,\alpha}^k(s) &= \frac{\sinh\left((l_1-\delta)v\right)}{\sinh\left(l_1 v\right)} \frac{\sinh\left((l_2-\delta)v\right)}{\sinh\left(l_2 v\right)} \widehat{e}_{1,\alpha}^{k-2}(s), \\ \widehat{e}_{2,\beta}^k(s) &= \frac{\sinh\left((l_1-\delta)v\right)}{\sinh\left(l_1 v\right)} \frac{\sinh\left((l_2-\delta)v\right)}{\sinh\left(l_2 v\right)} \widehat{e}_{2,\beta}^{k-2}(s), \end{aligned} \tag{2.11}$$

for $s \in R_s$, *where* $\delta = \beta - \alpha$, $l_1 = N + \beta$, *and* $l_2 = N - \alpha$.

Proof. Using (2.7) and (2.9), the Laplace transform of the error at the interfaces x_α and x_β can be written as

$$\begin{aligned} \widehat{e}_{1,\alpha}^k(s) &= \left(\lambda_+^{\alpha}, \lambda_+^{-\alpha}\right)\mathbf{c_1^k} = \left(\lambda_+^{\alpha}, \lambda_+^{-\alpha}\right)\Lambda_1^{-1}\Theta_1\mathbf{c_2^{k-1}}, \\ \widehat{e}_{2,\beta}^k(s) &= \left(\lambda_+^{\beta}, \lambda_+^{-\beta}\right)\mathbf{c_2^k} = \left(\lambda_+^{\beta}, \lambda_+^{-\beta}\right)\Lambda_2^{-1}\Theta_2\mathbf{c_1^{k-1}}. \end{aligned} \tag{2.12}$$

Substituting the matrices Λ_1, Λ_2, Θ_1 and Θ_2 from (2.10) gives

$$\widehat{e}_{1,\alpha}^k(s) = \frac{\lambda_+^{N+\alpha} - \lambda_+^{-(N+\alpha)}}{\lambda_+^{N+\beta} - \lambda_+^{-(N+\beta)}} \widehat{e}_{2,\beta}^{k-1}(s) \quad \text{and} \quad \widehat{e}_{2,\beta}^k(s) = \frac{\lambda_+^{N-\beta} - \lambda_+^{-(N-\beta)}}{\lambda_+^{N-\alpha} - \lambda_+^{-(N-\alpha)}} \widehat{e}_{1,\alpha}^{k-1}(s). \tag{2.13}$$

Using the mapping, $\lambda_+ = e^v$, the definition of the hyperbolic sine function, and substituting $\delta = \beta - \alpha$, $l_1 = N + \beta$, and $l_2 = N - \alpha$, we have

$$\widehat{e}^k_{1,\alpha}(s) = \frac{\sinh\left((l_1 - \delta)v\right)}{\sinh\left(l_1 v\right)}\widehat{e}^{k-1}_{2,\beta}(s) \quad \text{and} \quad \widehat{e}^k_{2,\beta}(s) = \frac{\sinh\left((l_2 - \delta)v\right)}{\sinh\left(l_2 v\right)}\widehat{e}^{k-1}_{1,\alpha}(s). \tag{2.14}$$

Using the expression for $\widehat{e}^{k-1}_{2,\beta}(s)$ and substituting into $\widehat{e}^k_{1,\alpha}(s)$ gives the first expression in (2.11). The second expression in (2.11) is obtained similarly. □

The quantities δ and l_j for $j = 1, 2$, in Lemma 2.8, determine the overlap and the subdomain sizes, respectively.

Remark. It is easy to see that as $N \to \infty$ (*i.e.* when recover an infinite spatial domain) the contraction rate for the error in (2.11) tends to $|\lambda_+|^{2(\alpha-\beta)}$ which exactly matches the result obtained by Wu and Al-Khaleel [26] when Dirichlet transmission conditions are used. We note further that (2.13) and (2.14) are generalizations of the corresponding expressions for the error on a bounded spatial domain found through continuous and a semi-discrete analyses in [24]. This allows us to directly compare our contraction rates to those found therein. In the semi-discrete case (as $\Delta t \to 0$ with Δx fixed), the contraction rate at the interfaces is given in (2.11) where v is replaced by

$$\tilde{v}(s, \Delta x) = \ln\left(1 + \frac{1}{2}s\Delta x^2 + \sqrt{\frac{1}{4}s^2\Delta x^4 + s\Delta x^2}\right).$$

We note here that using an inequality developed later in Lemma 2.12, we are easily able to show that this semi-discrete contraction rate is bounded above by the semi-discrete contraction rate obtained in [9]. And further, taking the limit of $\tilde{v}(s, \Delta x)$ as $\Delta x \to 0$ and making use of Lemma 2.12 we recover the continuous contraction rate obtained in [9].

To show that the moduli of the coefficients in the error recursion (2.11) are strictly less than one for all $s \in R_s$ a more detailed analysis of λ_+ is necessary.

Lemma 2.9. *If $\theta \in \left[\frac{1}{2}, 1\right]$ then the quantity $\eta = \frac{z-1}{\theta(z-1)+1}$ in the expression for λ_+ in (2.8) satisfies $Re(\eta) > 0$ and hence $Re(\lambda_+) > 1$.*

Proof. Consider $\eta = \frac{z-1}{\theta(z-1)+1}$ where $z = e^{s\Delta t}, s \in R_s$. The real part of η is given by

$$\mathrm{Re}(\eta) = \frac{\theta e^{2\Delta t\sigma} + (1-2\theta)e^{\Delta t\sigma}\cos(\Delta t\omega) + (\theta - 1)}{\left(\theta e^{\Delta t\sigma}\cos(\Delta t\omega) + (1-\theta)\right)^2 + \left(\theta e^{\Delta t\sigma}\sin(\Delta t\omega)\right)^2}. \tag{2.15}$$

The function $\mathrm{Re}(\eta)$ is well defined and positive for $\theta \in \left[\frac{1}{2}, 1\right]$. To see this, assume that

$$\left(\theta e^{\Delta t\sigma}\cos(\Delta t\omega) + (1-\theta)\right)^2 + \left(\theta e^{\Delta t\sigma}\sin(\Delta t\omega)\right)^2 = 0,$$

which requires

$$e^{\Delta t\sigma}\cos(\Delta t\omega) = \frac{\theta - 1}{\theta} \quad \text{and} \quad \sin(\Delta t\omega) = 0.$$

If $\sin(\Delta t\omega) = 0$ then $\omega \in \{0, \pm\pi/\Delta t\}$. Substituting $\omega \in \{0, \pm\pi/\Delta t\}$ into $e^{\Delta t\sigma}\cos(\Delta t\omega) = \frac{\theta-1}{\theta}$ forces

$$e^{\Delta t\sigma} = \pm\frac{\theta - 1}{\theta}. \tag{2.16}$$

Equation (2.16) has no solution. To see this, we first note that for $\sigma > 0$ we have $e^{\Delta t\sigma} > 1$. For $\theta \in [\frac{1}{2}, 1]$, we have $\frac{\theta-1}{\theta} \in [-1, 0]$ and $\frac{1-\theta}{\theta} \in [0, 1]$. Hence, $\left(\theta e^{\Delta t\sigma}\cos(\Delta t\omega) + (1-\theta)\right)^2 + \left(\theta e^{\Delta t\sigma}\sin(\Delta t\omega)\right)^2 > 0$.

Now we show $\theta e^{2\Delta t\sigma} + (1-2\theta)e^{\Delta t\sigma}\cos(\Delta t\omega) + (\theta-1) > 0$. Since $\cos(\Delta t\omega) \in [-1,1]$, for $|\omega| \le \pi/\Delta t$, and $1-2\theta \le 0$, for $\theta \in [\frac{1}{2},1]$, we have

$$\theta e^{2\Delta t\sigma} + (1-2\theta)e^{\Delta t\sigma}\cos(\Delta t\omega) + (\theta-1) \ge \theta e^{2\Delta t\sigma} + (1-2\theta)e^{\Delta t\sigma} + (\theta-1). \tag{2.17}$$

The right hand side of (2.17) is a quadratic function in $e^{\Delta t\sigma}$, is concave up for $\theta \in [\frac{1}{2},1]$, and has no roots. To see this, assume that $\theta e^{2\Delta t\sigma} + (1-2\theta)e^{\Delta t\sigma} + (\theta-1) = 0$. Factoring this gives the requirement

$$e^{\Delta t\sigma} = 1 \quad \text{and} \quad e^{\Delta t\sigma} = \frac{\theta-1}{\theta}. \tag{2.18}$$

The above equations have no solution since $\sigma > 0$ and $\theta \in [\frac{1}{2},1]$.

Since the numerator and the denominator of the right hand side of (2.15) are both positive, we have $\mathrm{Re}(\eta) > 0$. The real part of λ_+ defined in (2.8) is given by $\mathrm{Re}(\lambda_+) = 1 + \frac{\mathrm{Re}(\eta)}{2\mu} + \frac{\mathrm{Re}(\sqrt{\eta^2+4\mu\eta})}{2\mu}$. The conclusion $\mathrm{Re}(\lambda_+) > 1$ then follows from the fact that $\mathrm{Re}(\eta) > 0$ and the choice of the square root in λ_+. □

The following technical lemma will help us prove the main inequality in Lemma 2.12.

Lemma 2.10. *Suppose $\theta \in \left[\frac{1}{2},1\right]$. If $\lambda_+ = e^v$, then $Re(\cosh(v)) > 1$.*

Proof. Substituting $\lambda_+ = e^v$ into the quadratic equation $\lambda^2 - (2+\frac{\eta}{\mu})\lambda + 1 = 0$ and rearranging gives

$$\cosh(v) = 1 + \frac{\eta}{2\mu}. \tag{2.19}$$

From Lemma 2.9, we have $\mathrm{Re}(\eta) > 0$, from which the result follows. □

Lemma 2.11. *Suppose $\theta \in \left[\frac{1}{2},1\right]$. If $\lambda_+ = e^v$ where $v = x+iy$ then we have $x > 0$, $|y| < \frac{\pi}{2}$, and $|y| < x$.*

Proof. Due to periodicity, we may initially assume $y \in (-\pi,\pi]$. Using Euler's identity we have

$$\lambda_+ = e^v = e^x\cos(y) + ie^x\sin(y). \tag{2.20}$$

From Lemma 2.9, $\mathrm{Re}(\lambda_+) = e^x\cos(y) > 1$. Since $e^x > 0$ for all x, we must have $\cos(y) \in (0,1]$, this implies that $|y| < \frac{\pi}{2}$. Since $e^x\cos(y) > 1$ and $\cos(y) \in (0,1]$ we must have $x > 0$.

Now we show that $|y| < x$. We argue by contradiction. Suppose $0 < x \le |y| < \frac{\pi}{2}$. The cosine function is decreasing and $\cosh(x) > 1$ for $0 < x < \pi/2$. Hence we have $\cosh(x)\cos(y) \le \cosh(x)\cos(x)$. This implies $\cosh(x)\cos(y) < 1$, since $\cosh(x)\cos(x) < 1$ for $0 < x < \pi/2$. This contradicts the result in Lemma 2.10, where $\mathrm{Re}(\cosh(v)) = \cosh(x)\cos(y) > 1$. □

The image of the analytic complex function, $\lambda_+(v(s))$, $s \in R_s$, with $v = x+iy$, in the xy-plane is bounded for $\theta \in (1/2,1]$ and unbounded for $\theta = 1/2$, see Figure 3.

We can clearly see from the plots above that $x > 0$, $|y| < \frac{\pi}{2}$, and $|y| < x$ for $\theta \in [1/2,1]$.

Lemma 2.12. *Suppose $\theta \in \left[\frac{1}{2},1\right]$ and a, b are positive integers with $a < b$. If $\lambda_+ = e^v$, then for all $s \in R_s$ we have*

$$\left|\frac{\sinh(av)}{\sinh(bv)}\right| < \frac{a}{b}. \tag{2.21}$$

Moreover,

$$\sup_{s\in R_S}\left|\frac{\sinh(av(s))}{\sinh(bv(s))}\right| = \frac{a}{b}. \tag{2.22}$$

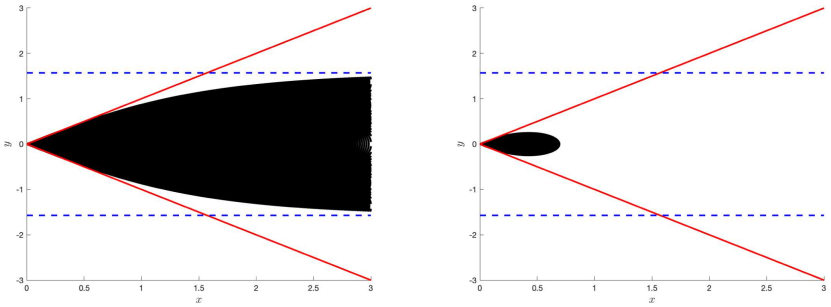

(a) (b)

FIGURE 3. The image of λ_+ on a semi-infinite time interval in the $xy-$plan for $\theta = 1/2$ (*left*) and for $\theta = 1$ (*right*). (a) $\theta = 1/2$ and (b) $\theta = 1$.

Proof. Let $v = x + iy$. Using trigonometric and hyperbolic identities, and with further simplification, we have

$$\left|\frac{\sinh(av)}{\sinh(bv)}\right|^2 = \frac{\cosh^2(ax) - \cos^2(ay)}{\cosh^2(bx) - \cos^2(by)}. \tag{2.23}$$

Using Taylor series

$$\begin{aligned}
\cosh^2(bx) - \cos^2(by) &= \left(1 + b^2x^2 + \frac{1}{3}b^4x^4 + \frac{2}{45}b^6x^6 + \frac{1}{315}b^8x^8 + \cdots\right) \\
&\quad - \left(1 - b^2y^2 + \frac{1}{3}b^4y^4 - \frac{2}{45}b^6y^6 + \frac{1}{315}b^8y^8 + \cdots\right) \\
&= b^2(x^2 + y^2) + \frac{1}{3}b^4(x^4 - y^4) + \frac{2}{45}b^6(x^6 + y^6) + \frac{1}{315}b^8(x^8 - y^8) + \cdots \\
&= \frac{b^2}{a^2}\left(a^2(x^2 + y^2) + \frac{1}{3}b^2a^2(x^4 - y^4) + \frac{2}{45}b^4a^2(x^6 + y^6) + \frac{1}{315}b^6a^2(x^8 - y^8) + \cdots\right).
\end{aligned}$$

From Lemma 2.11, $x > 0$ and $|y| < x$ in R_s, so all the terms in the above expression are positive. Using the assumption $b > a > 0$, we have

$$\begin{aligned}
\cosh^2(bx) - \cos^2(by) &> \frac{b^2}{a^2}\left(a^2(x^2 + y^2) + \frac{1}{3}a^4(x^4 - y^4) + \frac{2}{45}a^6(x^6 + y^6) + \frac{1}{315}a^8(x^8 - y^8) + \cdots\right) \\
&= \frac{b^2}{a^2}\left(\left(1 + a^2x^2 + \frac{1}{3}a^4x^4 + \frac{2}{45}a^6x^6 + \frac{1}{315}a^8x^8 + \cdots\right)\right. \\
&\quad \left. - \left(1 - a^2y^2 + \frac{1}{3}a^4y^4 - \frac{2}{45}a^6y^6 + \frac{1}{315}a^8y^8 + \cdots\right)\right) \\
&= \frac{b^2}{a^2}\left(\cosh^2(ax) - \cos^2(ay)\right).
\end{aligned}$$

Since $x > 0$, we have $\cosh^2(bx) - \cos^2(by) > 0$ and the result (2.21) follows.

To obtain the supremum in (2.22) we consider inequality (2.21) on the boundary of R_s. Indeed, it is easy to check that the inequality (and proof technique) holds if $|y| = x$, except at $x = 0$. Moreover, since a/b provides an upper bound on $|\sinh(av(s))/\sinh(bv(s))|$ for $s \in R_s$, $\lim_{|s|\to 0}|\sinh(av(s))/\sinh(bv(s))| = a/b$, and $\sinh(av(s))/\sinh(bv(s))$ is an analytic function for $s \in \bar{R}_s - (0,0)$, then (2.22) follows. □

Now we arrive at a convergence result on the interfaces x_α and x_β.

Lemma 2.13. *The Laplace transform of the errors in the approximations generated by the discrete SWR iteration (2.3) at the interfaces x_β and x_α satisfy*

$$\begin{aligned} \left|\widehat{e}^k_{1,\alpha}(s)\right| &\leq \frac{(l_1-\delta)}{l_1}\frac{(l_2-\delta)}{l_2}\left|\widehat{e}^{k-2}_{1,\alpha}(s)\right|, \\ \left|\widehat{e}^k_{2,\beta}(s)\right| &\leq \frac{(l_1-\delta)}{l_1}\frac{(l_2-\delta)}{l_2}\left|\widehat{e}^{k-2}_{2,\beta}(s)\right|, \end{aligned} \tag{2.24}$$

for all $s \in R_s$, where $\delta = \beta - \alpha$, $l_1 = N + \beta$, and $l_2 = N - \alpha$.

Proof. The proof of Lemma 2.13 follows directly from Lemmas 2.8 and 2.12. □

It is clear that for a fixed subdomain size the upper bound on the contraction rate, $\frac{(l_1-\delta)}{l_1}\frac{(l_2-\delta)}{l_2}$, improves as the overlap size, δ, increases.

Now we are in a position to prove the convergence of (2.3). First, we prove that the following maximum principle holds for the Laplace transforms of the error components.

Lemma 2.14. *Suppose $\theta \in \left[\frac{1}{2}, 1\right]$. If $\lambda_+ = e^v$, then the maximum error for the fully discrete two subdomain SWR iteration (2.3) occurs on the boundaries x_α and x_β. The Laplace transforms of the errors satisfy*

$$\begin{aligned} \left|\widehat{e}^k_{1,m}(s)\right| &< \left|\widehat{e}^{k-1}_{2,\beta}(s)\right|, \quad \text{for} \quad m = -N, \ldots, \beta - 1, \\ \left|\widehat{e}^k_{2,m}(s)\right| &< \left|\widehat{e}^{k-1}_{1,\alpha}(s)\right|, \quad \text{for} \quad m = \alpha + 1, \ldots, N, \end{aligned} \tag{2.25}$$

for all $s \in R_s$. On the exterior boundaries of the physical domain the error vanishes: $\widehat{e}^k_{1,-N}(s) = \widehat{e}^k_{2,N}(s) = 0$ for all $s \in R_s$.

Proof. Using (2.9), we have

$$\begin{aligned} \widehat{e}^k_{1,m}(s) &= \left(\lambda_+^m, \lambda_+^{-m}\right)\mathbf{c_1^k} = \left(\lambda_+^m, \lambda_+^{-m}\right)\Lambda_1^{-1}\Theta_1\mathbf{c_2^{k-1}}, \quad \text{for} \quad m = -N, \ldots, \beta, \\ \widehat{e}^k_{2,m}(s) &= \left(\lambda_+^m, \lambda_+^{-m}\right)\mathbf{c_2^k} = \left(\lambda_+^m, \lambda_+^{-m}\right)\Lambda_2^{-1}\Theta_2\mathbf{c_1^{k-1}}, \quad \text{for} \quad m = \alpha, \ldots, N. \end{aligned} \tag{2.26}$$

Simplifying (2.26) gives

$$\begin{aligned} \widehat{e}^k_{1,m}(s) &= \frac{\lambda_+^{N+m} - \lambda_+^{-(N+m)}}{\lambda_+^{N+\beta} - \lambda_+^{-(N+\beta)}}\widehat{e}^{k-1}_{2,\beta}(s), \quad \text{for} \quad m = -N, \ldots, \beta, \\ \widehat{e}^k_{2,m}(s) &= \frac{\lambda_+^{N-m} - \lambda_+^{-(N-m)}}{\lambda_+^{N-\alpha} - \lambda_+^{-(N-\alpha)}}\widehat{e}^{k-1}_{1,\alpha}(s), \quad \text{for} \quad m = \alpha, \ldots, N. \end{aligned} \tag{2.27}$$

Using the mapping, $\lambda_+ = e^v$, the expressions in (2.27) simplify to

$$\begin{aligned} \widehat{e}^k_{1,m}(s) &= \frac{\sinh((N+m)v)}{\sinh((N+\beta)v)}\widehat{e}^{k-1}_{2,\beta}(s), \quad \text{for} \quad m = -N, \ldots, \beta, \\ \widehat{e}^k_{2,m}(s) &= \frac{\sinh((N-m)v)}{\sinh((N-\alpha)v)}\widehat{e}^{k-1}_{1,\alpha}(s), \quad \text{for} \quad m = \alpha, \ldots, N. \end{aligned} \tag{2.28}$$

From Lemma 2.12, we have $\left|\frac{\sinh((N+m)v)}{\sinh((N+\beta)v)}\right| \leq 1$, for $m = -N, \ldots, \beta$, with a strict inequality if $m \neq \beta$ and $\left|\frac{\sinh((N-m)v)}{\sinh((N-\alpha)v)}\right| \leq 1$, for $m = \alpha, \ldots, N$, with a strict inequality if $m \neq \alpha$. Hence the result follows. □

Using Lemma 2.14, we now show the convergence of the fully discrete two subdomain SWR iteration, (2.3), at all nodes.

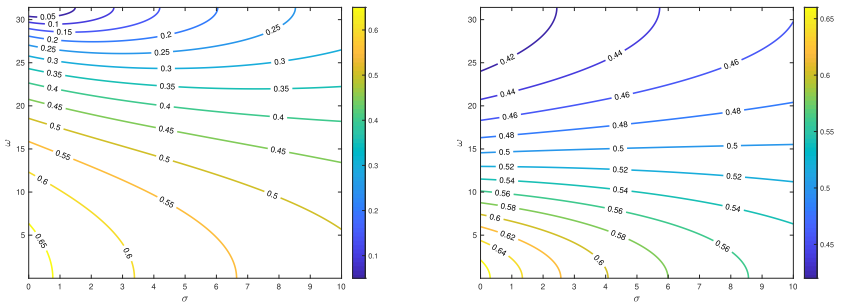

(a) (b)

FIGURE 4. Contour plot of the contraction rate, $\rho(s)$, from (2.31), for $\theta = 1/2$ (*left*) and $\theta = 1$ (*right*). (a) $\theta = 1/2$ and (b) $\theta = 1$.

Theorem 2.15. *Suppose $\theta \in \left[\frac{1}{2}, 1\right]$. The fully discrete two subdomain SWR iteration, (2.3), for the heat equation using the θ-method converges at a linear rate. The Laplace transform of the errors satisfy*

$$\begin{aligned} \left|\widehat{e}_{1,m}^{2k+1}(s)\right| &\leq \left(\frac{(l_1-\delta)}{l_1}\frac{(l_2-\delta)}{l_2}\right)^k \left|\widehat{e}_{2,\beta}^{0}(s)\right|, \quad \text{for} \quad m = -N,\ldots,\beta, \\ \left|\widehat{e}_{2,m}^{2k+1}(s)\right| &\leq \left(\frac{(l_1-\delta)}{l_1}\frac{(l_2-\delta)}{l_2}\right)^k \left|\widehat{e}_{1,\alpha}^{0}(s)\right|, \quad \text{for} \quad m = \alpha,\ldots,N, \end{aligned} \tag{2.29}$$

for all $s \in R_s$, where $\delta = \beta - \alpha$, $l_1 = N + \beta$, and $l_2 = N - \alpha$. Moreover, we have strict inequality in the first line of (2.29) if $m \neq \beta$ and in the second line if $m \neq \alpha$.

Proof. Using Lemma 2.14, we have

$$\begin{aligned} \left|\widehat{e}_{1,m}^{2k+1}(s)\right| &\leq \left|\widehat{e}_{2,\beta}^{2k}(s)\right|, \quad \text{for} \quad m = -N,\ldots,\beta, \\ \left|\widehat{e}_{2,m}^{2k+1}(s)\right| &\leq \left|\widehat{e}_{1,\alpha}^{2k}(s)\right|, \quad \text{for} \quad m = \alpha,\ldots,N. \end{aligned} \tag{2.30}$$

Now the result follows from Lemma 2.13 and induction. □

In the case $l_1 = l_2$, the result above was obtained in [18] using a different analysis and without providing an upper bound for the error.

Figure 4 shows contour plots of the contraction rate

$$\rho(s) = \left|\frac{\sinh\left((l_1-\delta)v\right)}{\sinh\left(l_1 v\right)}\frac{\sinh\left((l_2-\delta)v\right)}{\sinh\left(l_2 v\right)}\right|. \tag{2.31}$$

on two subdomains for $\theta = 1/2$ and $\theta = 1$. Here we choose $\Delta x = \Delta t = 0.1$ with a fixed overlap size of $\delta = 2$ and $l_1 = l_2 = 11$, corresponding to two subdomains $\Omega_1^{0.1} = \{-1,\ldots,0.1\}$ and $\Omega_2^{0.1} = \{-0.1,\ldots,1\}$. We plot the contour levels for the contraction rate on the top half of R_s, R_s^+. On the bottom half of R_s, R_s^-, the contraction rate behaves the same way. From Figure 4, for both $\theta = \frac{1}{2}$ and $\theta = 1$, we see that the contraction rate is strictly less than one in the $\sigma - \omega$ plane (defining R_s).

As a preview to the multidomain results in Section 3 we now formulate the iteration for the error on two subdomains as a matrix iteration, and obtain a convergence result in both the 2-norm and the infinity norm.

Lemma 2.16. *Suppose $\theta \in [\frac{1}{2}, 1]$. If $\lambda_+ = e^v$, then the error in the approximation generated by the two subdomain fully discrete SWR iteration at the interfaces x_α and x_β satisfies*

$$\xi^k = \mathbf{G}_2^2 \xi^{k-2}, \tag{2.32}$$

where $\xi^k = \left(\widehat{e}^k_{1,\alpha}, \widehat{e}^k_{2,\beta}\right)^T$,

$$\mathbf{G}_2^2 = \begin{pmatrix} r_1 p_2 & 0 \\ 0 & r_1 p_2 \end{pmatrix}, \tag{2.33}$$

and

$$r_1 = \frac{\sinh((l_1 - \delta)v)}{\sinh(l_1 v)}, \quad \text{and} \quad p_2 = \frac{\sinh((l_2 - \delta)v)}{\sinh(l_2 v)}. \tag{2.34}$$

Moreover,

$$\left\|\mathbf{G}_2^2\right\|_\infty = \left\|\mathbf{G}_2^2\right\|_2 = \left|\frac{\sinh((l_1 - \delta)v)}{\sinh(l_1 v)} \frac{\sinh((l_2 - \delta)v)}{\sinh(l_2 v)}\right| < \left|\frac{(l_1 - \delta)}{l_1} \frac{(l_2 - \delta)}{l_2}\right| < 1.$$

Parseval's identity for the discrete Laplace transform, in the next Lemma, will be useful to prove the convergence of the SWR algorithm in the time domain.

Lemma 2.17. *Let $v = (v(0), v(1), \ldots)^T$ be a general vector defined on a regular (time) grid with step size Δt. Then a Parseval's identity*

$$\sup_{\sigma>0} \int_{\frac{-\pi}{\Delta t}}^{\frac{\pi}{\Delta t}} |\widehat{v}(s)|^2 \mathrm{d}\omega = \Delta t \|v\|_2, \tag{2.35}$$

holds, where $\|v\|_2^2 = \sum_{n=0}^{\infty} |v(n)|^2$.

Moreover, if $v = (v(0), v(1), \ldots, v(T/\Delta t))^T$ then we have

$$\sup_{\sigma>0} \int_{\frac{\pi}{T} \le |\omega| \le \frac{\pi}{\Delta t}} |\widehat{v}(s)|^2 \mathrm{d}\omega = \frac{\Delta t}{T}(T - \Delta t)\|v\|_2, \tag{2.36}$$

where $\|v\|_2^2 = \sum_{n=0}^{T/\Delta t} |v(n)|^2$. Here, we assume that $T/\Delta t$ is an integer.

Proof. We will prove the first result (2.35), the second result (2.36) follows in a similar way. Substituting the discrete Laplace transform definition (2.5) into the left hand side of (2.35), we have

$$\int_{\frac{-\pi}{\Delta t}}^{\frac{\pi}{\Delta t}} |\widehat{v}(s)|^2 \mathrm{d}\omega = \frac{\Delta t^2}{2\pi} \sum_{n=0}^{\infty} \sum_{m=0}^{\infty} e^{-(n+m)\sigma\Delta t} v(n) v(m) \int_{\frac{-\pi}{\Delta t}}^{\frac{\pi}{\Delta t}} e^{i(m-n)\omega\Delta t} \mathrm{d}\omega. \tag{2.37}$$

The basis functions, $e^{ns\Delta t}$, in the double sums above are orthogonal over $\omega \in [-\pi/\Delta t, \pi/\Delta t]$, in fact

$$\int_{\frac{-\pi}{\Delta t}}^{\frac{\pi}{\Delta t}} e^{i(m-n)\omega\Delta t} \, \mathrm{d}\omega = \begin{cases} \frac{2\pi}{\Delta t} & n = m \\ 0 & n \neq m. \end{cases}$$

Now, we use the above orthogonality property to simplify the double sum in (2.37) and obtain

$$\int_{\frac{-\pi}{\Delta t}}^{\frac{\pi}{\Delta t}} |\widehat{v}(s)|^2 \, \mathrm{d}\omega = \Delta t \sum_{n=0}^{\infty} e^{-2n\sigma\Delta t} |v(n)|^2. \tag{2.38}$$

Taking the supremum of both sides in (2.38) over $\sigma > 0$ the result follows. □

The following corollary shows the convergence (at the interfaces) of the discrete SWR-algorithm in the time domain for $t > 0$.

Corollary 2.18. *Suppose $\theta \in [\frac{1}{2}, 1]$. If $\lambda_+ = e^v$, then the errors in the time domain at the interfaces x_α and x_β for $t > 0$, $\mathbf{e}^k_{1,\alpha}$ and $\mathbf{e}^k_{2,\beta}$, in the SWR approximation (2.3) converge and satisfy*

$$\begin{aligned} \left\|\mathbf{e}^k_{1,\alpha}\right\|_2 &\le \frac{(l_1-\delta)}{l_1}\frac{(l_2-\delta)}{l_2}\left\|\mathbf{e}^{k-2}_{1,\alpha}\right\|_2, \\ \left\|\mathbf{e}^k_{2,\beta}\right\|_2 &\le \frac{(l_1-\delta)}{l_1}\frac{(l_2-\delta)}{l_2}\left\|\mathbf{e}^{k-2}_{2,\beta}\right\|_2. \end{aligned} \tag{2.39}$$

Here $\|\mathbf{e}^k_{1,\alpha}\|_2^2 = \sum_{n=0}^{\infty}\left|e^k_{1,\alpha}(n)\right|^2$ and $\|\mathbf{e}^k_{2,\beta}\|_2^2 = \sum_{n=0}^{\infty}\left|e^k_{2,\beta}(n)\right|^2$.

Proof. The proof of Corollary 2.18 follows from Lemma 2.13 and Parseval's identity (2.35). □

The convergence in the time domain at all the interior nodes follows from convergence at the interfaces, x_α and x_β, Corollary 2.18, and a discrete maximum principle in the time domain.

In practice, we integrate in time using θ-method over a bounded time interval $t \in (0, T]$. This allows exchanging information between the subdomains at the end of the time interval T. The following corollary shows the convergence of the discrete SWR-algorithm (2.3) at the interfaces (in the time domain) on a bounded time interval $t \in (0, T]$.

Corollary 2.19. *Suppose $\theta \in [\frac{1}{2}, 1]$. If $\lambda_+ = e^v$, then the error in the SWR approximation (2.3) in the time domain $t \in (0, T]$ at the interfaces x_α and x_β, $\tilde{\mathbf{e}}^k_{1,\alpha}$ and $\tilde{\mathbf{e}}^k_{\mathbf{2},\beta}$, converge according to*

$$\begin{aligned} \left\|\tilde{\mathbf{e}}^k_{1,\alpha}\right\|_2 &\le \sup_{\tilde{R}_s}\left|\frac{\sinh\left((l_1-\delta)v\right)}{\sinh\left(l_1 v\right)}\frac{\sinh\left((l_2-\delta)v\right)}{\sinh\left(l_2 v\right)}\right|\left\|\tilde{\mathbf{e}}^{k-2}_{1,\alpha}\right\|_2, \\ \left\|\tilde{\mathbf{e}}^k_{2,\beta}\right\|_2 &\le \sup_{\tilde{R}_s}\left|\frac{\sinh\left((l_1-\delta)v\right)}{\sinh\left(l_1 v\right)}\frac{\sinh\left((l_2-\delta)v\right)}{\sinh\left(l_2 v\right)}\right|\left\|\tilde{\mathbf{e}}^{k-2}_{2,\beta}\right\|_2, \end{aligned} \tag{2.40}$$

where $\tilde{R}_s = \{s \,|\, s = \sigma + i\omega,\ \sigma > 0 \text{ and } \pi/T \le |\omega| \le \pi/\Delta t\}$, $\|\tilde{\mathbf{e}}^k_{1,\alpha}\|_2^2 = \sum_{n=0}^{T/\Delta t}\left|e^k_{1,\alpha}(n)\right|^2$ and $\|\tilde{\mathbf{e}}^k_{2,\beta}\|_2^2 = \sum_{n=0}^{T/\Delta t}\left|e^k_{2,\beta}(n)\right|^2$. Here, we assume that $T/\Delta t$ is an integer.

Proof. The proof of Corollary 2.19 follows by restricting the frequencies considered in Lemma 2.13 to $\pi/T \le |\omega| \le \pi/\Delta t$ and using Parseval's identity (2.36). □

Corollary 2.19 will be used to present the numerical results for the two subdomain case in the time domain in Section 4.

3. Multidomain convergence analysis

In this section, we discuss the fully discrete convergence analysis of the SWR-algorithm on arbitrary number of a bounded subdomains.

To obtain the classical SWR solution of (1.1) on an arbitrary (finite) number of subdomains, we decompose Ω into S overlapping subdomains: $\Omega_j^h = \{x_i : i = \alpha_j, \ldots, \beta_j\}$ for $j = 1, \ldots, S$ where $x_{\alpha_1} = -L$, $x_{\beta_S} = L$, and $x_{\alpha_{j+1}} < x_{\beta_j}$ for $j = 1, \ldots, S-1$. We assume that $x_{\beta_j} < x_{\alpha_{j+2}}$ for $j = 1, \ldots, S-2$ so that non-adjacent subdomains do not overlap, see Figure 5.

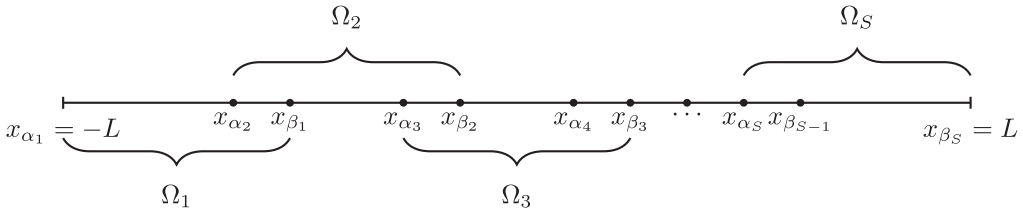

FIGURE 5. Multi-domain spatial decomposition.

The classical semi-discrete SWR algorithm on S subdomains, Ω_j^h, for $j = 1, \ldots, S$, can be written as: for $k = 1, 2, \ldots$, solve

$$\frac{\mathrm{d}\mathbf{u}_j^k(t)}{\mathrm{d}t} = A_j \mathbf{u}_j^k(t) + \mathbf{f}_j^k(t), \qquad t > 0, \tag{3.1}$$

where

$$\mathbf{u}_j^k(t) = \left(u_{j,(\alpha_j-1)}^k(t), u_{j,(\alpha_j-2)}^k(t), \ldots, u_{j,(\beta_j-1)}^k(t)\right)^T, \tag{3.2}$$

are the subdomain iterates on the interior nodes of Ω_j^h. Here, $A_j = \frac{1}{\Delta x^2}\text{tridiag}(1, -2, 1)$, where $A_j \in \mathbb{R}^{(\beta_j-\alpha_j-1)\times(\beta_j-\alpha_j-1)}$, for $j = 1, \ldots, S$.

The vectors $\mathbf{f}_j^k \in \mathbb{R}^{\beta_j-\alpha_j-1}$, for $j = 1, \ldots, S$, are defined by

$$\begin{aligned}
\mathbf{f}_1^k(t) &= \bar{\mathbf{f}}_1(t) + \frac{1}{\Delta x^2} u_{1,\beta_1}^k(t)\delta_{\mathbf{1},\mathbf{1}}, \\
\mathbf{f}_j^k(t) &= \bar{\mathbf{f}}_j(t) + \frac{1}{\Delta x^2} u_{j,\beta_j}^k(t)\delta_{\mathbf{1},\mathbf{j}} + \frac{1}{\Delta x^2} u_{j,\alpha_j}^k(t)\delta_{\mathbf{2},\mathbf{j}}, \qquad \text{for } j = 2, \ldots, S-1, \\
\mathbf{f}_S^k(t) &= \bar{\mathbf{f}}_S(t) + \frac{1}{\Delta x^2} u_{S,\alpha_S}^k(t)\delta_{\mathbf{2},\mathbf{S}},
\end{aligned} \tag{3.3}$$

where $\delta_{\mathbf{1},\mathbf{j}} \in \mathbb{R}^{\beta_j-\alpha_j-1}$ and $\delta_{\mathbf{2},\mathbf{j}} \in \mathbb{R}^{\beta_j-\alpha_j-1}$, are the unit column vectors

$$\delta_{\mathbf{1},\mathbf{j}} = (0, \ldots, 0, 1)^T \quad \text{and} \quad \delta_{\mathbf{2},\mathbf{j}} = (1, 0, \ldots, 0)^T. \tag{3.4}$$

The overbar notation indicates that $\bar{\mathbf{f}}_j$, for $j = 1, \ldots, S$, are components $\{\alpha_j + 1, \ldots, \beta_j - 1\}$ of $\mathbf{f}_j$. This bar notation will be used in this manner throughout this section.

The system (3.1) is supplemented with an initial condition

$$\mathbf{u}_j^k(0) = \bar{\mathbf{u}}_j(0), \qquad j = 1, \ldots, S, \tag{3.5}$$

and boundary and Dirichlet transmission conditions

$$\begin{aligned}
u_{1,\alpha_1}^k(t) &= h_1(t), & u_{1,\beta_1}^k(t) &= u_{2,\beta_1}^{k-1}(t), \\
u_{j,\alpha_j}^k(t) &= u_{j-1,\alpha_j}^{k-1}(t), & u_{j,\beta_j}^k(t) &= u_{j+1,\beta_j}^{k-1}(t), \quad \text{for } j = 2, \ldots, S-1, \\
u_{S,\alpha_S}^k(t) &= u_{S-1,\alpha_S}^{k-1}(t), & u_{S,\beta_S}^k(t) &= h_2(t).
\end{aligned} \tag{3.6}$$

Here, $u_{j,m}^k(t), t > 0$, represents the numerical approximation of $u(x,t)$ at $x = x_m$ on Ω_j^h obtained by the k^{th} iteration of the SWR algorithm. To get the iteration started, we must pick initial guesses for $u_{j,\beta_j}^0(t)$ and $u_{j,\alpha_j}^0(t)$, for $j = 1, \ldots, S$.

To analyze the fully discrete SWR algorithm we begin with a lemma which describes the single domain discrete solution of (1.1) on S subdomains using the θ-method.

Lemma 3.1. *The single domain solution at $t = t_n$, $\mathbf{u}(n)$, restricted to the interior of Ω_j^h, $\bar{\mathbf{u}}_j(n)$, for $j = 1, \ldots, S$, using the θ-method to integrate the semi-discrete heat equation (1.1), is the unique solution of the subsystems*

$$(I_j - \theta\Delta t A_j)\bar{\mathbf{u}}_\mathbf{j}(n) - \theta\Delta t\mathbf{f}_\mathbf{j}(n) = (I_j - (\theta-1)\Delta t A_j)\bar{\mathbf{u}}_\mathbf{j}(n-1) - (\theta-1)\Delta t\mathbf{f}_\mathbf{j}(n-1),$$

for $n = 1, 2, \ldots$, where

$$\begin{aligned}
\mathbf{f}_1(n) &= \bar{\mathbf{f}}_1(n) + \frac{1}{\Delta x^2}u_{\beta_1}(n)\delta_{\mathbf{1},\mathbf{1}},\\
\mathbf{f}_j(n) &= \bar{\mathbf{f}}_j(n) + \frac{1}{\Delta x^2}u_{\beta_j}(n)\delta_{\mathbf{1},\mathbf{j}} + \frac{1}{\Delta x^2}u_{\alpha_j}(n)\delta_{\mathbf{2},\mathbf{j}}, \quad \text{for } j = 2, \ldots, S-1,\\
\mathbf{f}_S(n) &= \bar{\mathbf{f}}_S(n) + \frac{1}{\Delta x^2}u_{\alpha_S}(n)\delta_{\mathbf{2},\mathbf{S}}.
\end{aligned} \tag{3.7}$$

Here $\mathbf{f}_j(n) = \mathbf{f}_j(t_n)$, for $j = 1, \ldots, S$, $\delta_{\mathbf{1},\mathbf{j}}$ and $\delta_{\mathbf{2},\mathbf{j}}$, for $j = 1, \ldots, S$, are defined in (3.4). The quantities $u_{\beta_j}(n)$ and $u_{\alpha_j}(n)$, for $j = 1, \ldots, S$, are the single domain solutions at the interface nodes at time t_n, and I_j, for $j = 1, \ldots, S$, are the $(\beta_j - \alpha_j - 1) \times (\beta_j - \alpha_j - 1)$ identity matrices.

Similar expressions for the SWR approximations are given in the next lemma.

Lemma 3.2. *The solution of (3.1)–(3.6) using the θ-method at $t = t_n$, $\mathbf{u}_j^k(n)$, for $j = 1, \ldots, S$, are the unique solutions of the subsystems*

$$(I_j - \theta\Delta t A_j)\mathbf{u}_\mathbf{j}^\mathbf{k}(n) - \theta\Delta t\mathbf{f}_\mathbf{j}^\mathbf{k}(n) = (I_j - (\theta-1)\Delta t A_j)\mathbf{u}_\mathbf{j}^\mathbf{k}(n-1) - (\theta-1)\Delta t\mathbf{f}_\mathbf{j}^\mathbf{k}(n-1), \tag{3.8}$$

for $n = 1, 2, \ldots$. Here $\mathbf{f}_j^k(n) \equiv \mathbf{f}_j^k(t_n)$, for $j = 1, \ldots, S$, where the vectors $\mathbf{f}_j^k(t)$ are defined in (3.3).

We denote the error between the single domain and SWR solutions at time step n by $\mathbf{e}_j^k(n) = \mathbf{u}_j^k(n) - \bar{\mathbf{u}}_j(n)$ for $j = 1, \ldots, S$. Simply subtracting the representations of the single domain and SWR solutions, from the previous two lemmas, gives the following result.

Lemma 3.3. *For $k = 1, 2, \ldots$ and $n = 1, 2, \ldots$, the errors, $\mathbf{e}_j^k(n)$, for $j = 1, \ldots, S$ in the SWR approximations from (3.8) satisfy*

$$\begin{aligned}
(I_1 - \theta\Delta t A_1)\mathbf{e}_\mathbf{1}^\mathbf{k}(n) - \mu\theta e_{1,\beta_1}^k(n)\delta_{\mathbf{1},\mathbf{1}} &= (I_1 - (\theta-1)\Delta t A_1)\mathbf{e}_\mathbf{1}^\mathbf{k}(n-1) - \mu(\theta-1)e_{1,\beta_1}^k(n-1)\delta_{\mathbf{1},\mathbf{1}},\\
(I_j - \theta\Delta t A_j)\mathbf{e}_\mathbf{j}^\mathbf{k}(n) - \mu\theta\Big(e_{j,\beta_j}^k(n)\delta_{\mathbf{1},\mathbf{j}} + e_{j,\alpha_j}^k(n)\delta_{\mathbf{2},\mathbf{j}}\Big) &= (I_j - (\theta-1)\Delta t A_j)\mathbf{e}_\mathbf{j}^\mathbf{k}(n-1)\\
&\quad - \mu(\theta-1)\Big(e_{j,\beta_j}^k(n-1)\delta_{\mathbf{1},\mathbf{j}} + e_{j,\alpha_j}^k(n-1)\delta_{\mathbf{2},\mathbf{j}}\Big),\\
&\quad j = 2, \ldots, S-1\\
(I_S - \theta\Delta t A_S)\mathbf{e}_\mathbf{S}^\mathbf{k}(n) - \mu\theta e_{S,\alpha_S}^k(n)\delta_{\mathbf{2},\mathbf{S}} &= (I_S - (\theta-1)\Delta t A_S)\mathbf{e}_\mathbf{S}^\mathbf{k}(n-1) - \mu(\theta-1)e_{S,\alpha_S}^k(n-1)\delta_{\mathbf{2},\mathbf{S}},
\end{aligned}$$

with initial condition

$$\mathbf{e}_j^k(0) = \bar{\mathbf{0}}_j, \quad \text{for } j = 1, \ldots, S,$$

and boundary and transmission conditions given by

$$\begin{aligned}
e_{1,\alpha_1}^k(n) &= 0, & e_{1,\beta_1}^k(n) &= e_{2,\beta_1}^{k-1}(n),\\
e_{j,\alpha_j}^k(n) &= e_{j-1,\alpha_j}^{k-1}(n), & e_{j,\beta_j}^k(n) &= e_{j+1,\beta_j}^{k-1}(n), \quad \text{for } j = 2, \ldots, S-1,\\
e_{S,\alpha_S}^k(n) &= e_{S-1,\alpha_S}^{k-1}(n), & e_{S,\beta_S}^k(n) &= 0.
\end{aligned} \tag{3.9}$$

Here, $\mu = \Delta t/\Delta x^2$ and $\bar{\mathbf{0}}_\mathbf{j} \in \mathbb{R}^{\beta_j - \alpha_j - 1}$, for $j = 1, \ldots, S$, is a zero vector.

Using the boundary values and the definitions of A_j, $\delta_{\mathbf{1,j}}$, and $\delta_{\mathbf{2,j}}$, for $j = 1, \ldots, S$, we obtain the following lemma.

Lemma 3.4. *Component-wise, for $j = 1, \ldots, S$, $k = 1, 2, \ldots$ and $n = 1, 2, \ldots$ the errors, $\mathbf{e}^k_{j,m_j}(n)$, in the SWR approximations obtained in (3.8) satisfy*

$$-\mu\theta e^k_{j,m_j-1}(n) + (1+2\mu\theta)e^k_{j,m_j}(n) - \mu\theta e^k_{j,m_j+1}(n) = -\mu(\theta-1)e^k_{j,m_j-1}(n-1) + (1+2\mu(\theta-1))e^k_{j,m_j}(n-1) - \mu(\theta-1)e^k_{j,m_j+1}(n-1),$$

where $m_j \in \{\alpha_j + 1, \ldots, \beta_j - 1\}$, subject to $e^k_{j,m_j}(0) = 0$ and (3.9).

The recursions for the discrete Laplace transforms of the errors are recorded in the next lemma.

Lemma 3.5. *For $j = 1, \ldots, S$, $k = 1, 2, \ldots$ and $n = 1, 2, \ldots$, the discrete Laplace transform of errors, $\widehat{\mathbf{e}}^k_{j,m_j}(n)$, in the SWR approximations obtained from (3.8) satisfy*

$$\mu\widehat{e}^k_{j,m_j-1}(s) - (2\mu+\eta)\widehat{e}^k_{j,m_j}(s) + \mu\widehat{e}^k_{j,m_j+1}(s) = 0, \tag{3.10}$$

where $m_j \in \{\alpha_j + 1, \ldots, \beta_j - 1\}$, $\mu = \Delta t/\Delta x^2$, $\eta = \frac{z-1}{\theta(z-1)+1}$ and $z = e^{s\Delta t}$, for $s \in R_s$. The Laplace transforms of the boundary conditions are

$$\begin{aligned}
&\widehat{e}^k_{1,\alpha_1}(s) = 0, && \widehat{e}^k_{1,\beta_1}(s) = \widehat{e}^{k-1}_{2,\beta_1}(s),\\
&\widehat{e}^k_{j,\alpha_j}(s) = \widehat{e}^{k-1}_{j-1,\alpha_j}(s), && \widehat{e}^k_{j,\beta_j}(s) = \widehat{e}^{k-1}_{j+1,\beta_j}(s), \quad \text{for } j = 2, \ldots, S-1,\\
&\widehat{e}^k_{S,\alpha_S}(s) = \widehat{e}^{k-1}_{S-1,\alpha_S}(s), && \widehat{e}^k_{S,\beta_S}(s) = 0.
\end{aligned} \tag{3.11}$$

The general solutions of these recursion relations are given in the next two lemmas.

Lemma 3.6. *The general solutions of the recursions (3.10) and (3.11) for the Laplace transforms of the error are given by*

$$\widehat{e}^k_{j,m_j}(s) = a^k_j\lambda_+^{m_j} + b^k_j\lambda_+^{-m_j}, \quad \text{for } m_j \in \{\alpha_j + 1, \ldots, \beta_j - 1\}, \quad \text{and } j = 1, \ldots, S, \tag{3.12}$$

where λ_+ solves $\lambda^2 - (2 + \frac{\eta}{\mu})\lambda + 1 = 0$ and is given explicitly by

$$\lambda_+ = 1 + \frac{\eta}{2\mu} + \frac{\sqrt{\eta^2 + 4\mu\eta}}{2\mu}, \tag{3.13}$$

where $\mu = \frac{\Delta t}{\Delta x^2}$, $\eta = \frac{z-1}{\theta(z-1)+1}$ and $z = e^{s\Delta t}, s \in R_s$. In the expression for λ_+, we have chosen the square root with positive real part.

The coefficients $(a^k_j, b^k_j)^T =: \mathbf{c}^k_j$ in the representations of the errors above are shown to satisfy a fixed point iteration in the next lemma.

Lemma 3.7. *The coefficients $\mathbf{c}^k_j = (a^k_j, b^k_j)^T$, for $j = 1, \ldots, S$, in the general solution for the Laplace transforms of the errors, satisfy*

$$\begin{aligned}
\mathbf{c^k_1} &= \Lambda_1^{-1}\Pi_1\mathbf{c^{k-1}_2},\\
\mathbf{c^k_j} &= \Lambda_j^{-1}\Theta_j\mathbf{c^{k-1}_{j-1}} + \Lambda_j^{-1}\Pi_j\mathbf{c^{k-1}_{j+1}}, \quad \text{for } j = 2, \ldots, S-1,\\
\mathbf{c^k_S} &= \Lambda_S^{-1}\Theta_S\mathbf{c^{k-1}_{S-1}},
\end{aligned} \tag{3.14}$$

where

$$\Lambda_j = \begin{pmatrix} \lambda_+^{\alpha_j} & \lambda_+^{-\alpha_j} \\ \lambda_+^{\beta_j} & \lambda_+^{-\beta_j} \end{pmatrix}, \quad \Theta_j = \begin{pmatrix} \lambda_+^{\alpha_j} & \lambda_+^{-\alpha_j} \\ 0 & 0 \end{pmatrix}, \quad \text{and} \quad \Pi_j = \begin{pmatrix} 0 & 0 \\ \lambda_+^{\beta_j} & \lambda_+^{-\beta_j} \end{pmatrix}. \tag{3.15}$$

Proof. Using the expression (3.12) and the boundary and transmission conditions (3.11) we have

$$\begin{aligned}
&a_1^k\lambda_+^{\alpha_1} + b_1^k\lambda_+^{-\alpha_1} = 0, && a_1^k\lambda_+^{\beta_1} + b_1^k\lambda_+^{-\beta_1} = a_2^{k-1}\lambda_+^{\beta_1} + b_2^{k-1}\lambda_+^{-\beta_1},\\
&a_j^k\lambda_+^{\alpha_j} + b_j^k\lambda_+^{-\alpha_j} = a_{j-1}^{k-1}\lambda_+^{\alpha_j} + b_{j-1}^{k-1}\lambda_+^{-\alpha_j}, && a_j^k\lambda_+^{\beta_j} + b_j^k\lambda_+^{-\beta_j} = a_{j+1}^{k-1}\lambda_+^{\beta_j} + b_{j+1}^{k-1}\lambda_+^{-\beta_j}, \quad \text{for } j = 2,\dots,S-1,\\
&a_S^k\lambda_+^{\alpha_S} + b_S^k\lambda_+^{-\alpha_S} = a_{S-1}^{k-1}\lambda_+^{\alpha_S} + b_{S-1}^{k-1}\lambda_+^{-\alpha_S}, && a_S^k\lambda_+^{\beta_S} + b_S^k\lambda_+^{-\beta_S} = 0.
\end{aligned} \tag{3.16}$$

Writing (3.16) in matrix form we have

$$\begin{aligned}
&\Lambda_1\mathbf{c_1^k} = \Pi_1\mathbf{c_2^{k-1}},\\
&\Lambda_j\mathbf{c_j^k} = \Theta_j\mathbf{c_{j-1}^{k-1}} + \Pi_j\mathbf{c_{j+1}^{k-1}}, \quad \text{for } j = 2,\dots,S-1,\\
&\Lambda_S\mathbf{c_S^k} = \Theta_S\mathbf{c_{S-1}^{k-1}},
\end{aligned} \tag{3.17}$$

where Λ_j, Θ_j, and Π for $j = 1,\dots,S$, are defined in (3.15). Multiplying each equality in (3.17) by the inverse of Λ_j, for $j = 1,\dots,S$, the result follows. □

A straightforward, but slightly tedious calculation, gives the following iteration for the vector of Laplace transforms of the errors at the interfaces.

Lemma 3.8. *If $\lambda_+ = e^v$, then the Laplace transforms of the errors in the approximation generated by the fully discrete multi-domain SWR iteration (3.8) at the interfaces x_{β_j}, for $j = 1,\dots,S-1$, and x_{α_j}, for $j = 2,\dots,S$, satisfy*

$$\xi^k = \mathbf{G}_S\xi^{k-1}, \tag{3.18}$$

where

$$\xi^k = \left(\widehat{e}_{1,\alpha_2}^k(s), \widehat{e}_{2,\beta_1}^k(s), \widehat{e}_{2,\alpha_3}^k(s), \dots, \widehat{e}_{S-1,\beta_{S-2}}^k(s), \widehat{e}_{S-1,\alpha_S}^k(s), \widehat{e}_{S,\beta_S-1}^k(s)\right)^T, \tag{3.19}$$

$s \in R_s$, and $\mathbf{G}_S \in \mathbb{C}^{2(S-1)\times 2(S-1)}$ is given by

$$\mathbf{G}_S = \begin{pmatrix}
0 & r_1 & & & & & & & \\
p_2 & 0 & 0 & q_2 & & & & & \\
s_2 & 0 & 0 & r_2 & & & & & \\
 & & p_3 & 0 & 0 & q_3 & & & \\
 & & s_3 & 0 & 0 & r_3 & & & \\
 & & & \ddots & \ddots & \ddots & \ddots & & \\
 & & & & & & p_{S-1} & 0 & 0 & q_{S-1}\\
 & & & & & & s_{S-1} & 0 & 0 & r_{S-1}\\
 & & & & & & & p_S & 0 &
\end{pmatrix} \tag{3.20}$$

The non-zero elements in the matrix are

$$\begin{aligned}
r_j &= \frac{\sinh((l_j-\delta_j)v)}{\sinh(l_jv)}, && \text{for } j = 1,\dots,S-1,\\
p_j &= \frac{\sinh((l_j-\delta_{j-1})v)}{\sinh(l_jv)}, && \text{for } j = 2,\dots,S,\\
q_j &= \frac{\sinh(\delta_{j-1}v)}{\sinh(l_jv)}, && \text{for } j = 2,\dots,S-1,\\
s_j &= \frac{\sinh(\delta_jv)}{\sinh(l_jv)}, && \text{for } j = 2,\dots,S-1.
\end{aligned} \tag{3.21}$$

The quantities $\delta_j = \beta_j - \alpha_{j+1}$, for $j = 1,\dots,S-1$, and $l_j = \beta_j - \alpha_j$, for $j = 1,\dots,S$, determine the overlaps and the subdomain sizes, respectively.

Proof. On Ω_1, using (3.14), the Laplace transform of the error on the interface x_{α_2}, can be written as

$$\widehat{e}^{k}_{1,\alpha_2}(s) = \left(\lambda_+^{\alpha_2}, \lambda_+^{-\alpha_2}\right)\mathbf{c_1^k} = \left(\lambda_+^{\alpha_2}\ \lambda_+^{-\alpha_2}\right)\Lambda_1^{-1}\Pi_1\mathbf{c_2^{k-1}}. \tag{3.22}$$

Substituting in the elements of the matrices Λ_1 and Π_1, using hyperbolic identities, using the mapping $\lambda_+ = e^v$, and introducing the quantities $\delta_1 = \beta_1 - \alpha_2$ and $l_1 = \beta_1 - \alpha_1$, we have

$$\widehat{e}^{k}_{1,\alpha_2}(s) = \frac{\sinh\left((l_1-\delta_1)v\right)}{\sinh\left(l_1 v\right)}\widehat{e}^{k-1}_{2,\beta_1}(s) = r_1\widehat{e}^{k-1}_{2,\beta_1}(s), \tag{3.23}$$

where r_1 is defined in (3.21).

On Ω_j, for $j = 2, \ldots, S-1$, using (3.14), the mapping $\lambda_+ = e^v$, and introducing the quantities $\delta_j = \beta_j - \alpha_{j+1}$ and $l_j = \beta_j - \alpha_j$, we may write the Laplace transforms of the errors on the interfaces $x_{\beta_{j-1}}$ and $x_{\alpha_{j+1}}$ as

$$\begin{aligned}
\widehat{e}^{k}_{j,\beta_{j-1}}(s) &= \frac{\sinh\left((l_j-\delta_{j-1})v\right)}{\sinh\left(l_j v\right)}\widehat{e}^{k-1}_{j-1,\alpha_j}(s) + \frac{\sinh\left(\delta_{j-1}v\right)}{\sinh\left(l_j v\right)}\widehat{e}^{k-1}_{j+1,\beta_j}(s) = p_j\widehat{e}^{k-1}_{j-1,\alpha_j}(s) + q_j\widehat{e}^{k-1}_{j+1,\beta_j}(s),\\
\widehat{e}^{k}_{j,\alpha_{j+1}}(s) &= \frac{\sinh\left(\delta_j v\right)}{\sinh\left(l_j v\right)}\widehat{e}^{k-1}_{j-1,\alpha_j}(s) + \frac{\sinh\left((l_j-\delta_j)v\right)}{\sinh\left(l_j v\right)}\widehat{e}^{k-1}_{j+1,\beta_j}(s) = s_j\widehat{e}^{k-1}_{j-1,\alpha_j}(s) + r_j\widehat{e}^{k-1}_{j+1,\beta_j}(s).
\end{aligned} \tag{3.24}$$

where p_j, q_j, s_j, and r_j are defined in (3.21).

Finally, on Ω_S, using (3.14) and introducing the quantities $\delta_{S-1} = \beta_{S-1} - \alpha_S$ and $l_S = \beta_S - \alpha_S$, we have the Laplace transform of the error on the interface $x_{\beta_{S-1}}$ as

$$\widehat{e}^{k}_{S,\beta_{S-1}}(s) = \frac{\sinh\left((l_S-\delta_{S-1})v\right)}{\sinh\left(l_S v\right)}\widehat{e}^{k-1}_{S-1,\alpha_S}(s) = p_S\widehat{e}^{k-1}_{S-1,\alpha_S}(s), \tag{3.25}$$

where p_S is defined in (3.21).

Writing (3.23), (3.25), and (3.24) in matrix form we arrive at (3.18). □

The next lemma proves the convergence at the interfaces in the infinity norm.

Lemma 3.9. *Suppose $\theta \in [\frac{1}{2}, 1]$. The Laplace transforms of the errors defined in (3.18) converge to the zero vector as $k \to \infty$ in the infinity norm.*

Proof. The infinity norm of $\mathbf{G}_S$ is

$$\|\mathbf{G}_S\|_\infty = \max\left\{|r_1|, |p_S|, \max_{j=2,\ldots,S-1}\{|p_j| + |q_j|, |s_j| + |r_j|\}\right\}, \tag{3.26}$$

where p_j, q_j, s_j, and r_j are defined in (3.21). Using Lemma 2.12, for all $s \in R_s$, we have

$$\begin{aligned}
|r_1| &= \left|\frac{\sinh((l_1-\delta_1)v)}{\sinh(l_1 v)}\right| < \frac{l_1-\delta_1}{l_1} < 1,\\
|p_S| &= \left|\frac{\sinh((l_S-\delta_{S-1})v)}{\sinh(l_S v)}\right| < \frac{l_S-\delta_{S-1}}{l_S} < 1,\\
|p_j| + |q_j| &= \left|\frac{\sinh((l_j-\delta_{j-1})v)}{\sinh(l_j v)}\right| + \left|\frac{\sinh(\delta_{j-1}v)}{\sinh(l_j v)}\right| < \frac{l_j-\delta_{j-1}}{l_j} + \frac{\delta_{j-1}}{l_j} = 1,\\
|s_j| + |r_j| &= \left|\frac{\sinh(\delta_j v)}{\sinh(l_j v)}\right| + \left|\frac{\sinh((l_j-\delta_j)v)}{\sinh(l_j v)}\right| < \frac{\delta_j}{l_j} + \frac{l_j-\delta_j}{l_j} = 1.
\end{aligned} \tag{3.27}$$

From (3.26) and (3.27), we have $\|\mathbf{G}_S\|_\infty < 1$, and the result follows. □

Remark. We see that the infinity norm of $\mathbf{G}$ will tend to one if even a single overlap shrinks to zero, which coincides with our usual understanding of the convergence of (classical) Schwarz methods.

The following lemma is used to prove that a maximum principle holds in the fully discrete multi-domain case.

Lemma 3.10. *Suppose $m_j \in \{\alpha_j, \dots, \beta_j\}$, for $j = 1, \dots, S$, and define*

$$\zeta^k = \left(\widehat{e}^k_{1,m_1}(s), \widehat{e}^k_{2,m_2}(s), \dots, \widehat{e}^k_{S-1,m_{S-1}}(s), \widehat{e}^k_{S,m_S}(s)\right)^T, \tag{3.28}$$

where $\widehat{e}^k_{j,m_j}$ is the Laplace transform of the SWR error at an arbitrary node $m_j \in \Omega_j$. If $\lambda_+ = e^v$, then

$$\zeta^k = \mathbf{G}^*_S \xi^{k-1}, \tag{3.29}$$

where ξ^k is defined in (3.19) and $\mathbf{G}^*_S \in \mathbb{C}^{S\times 2(S-1)}$ is given by

$$\mathbf{G}^*_S = \begin{pmatrix} 0 & q^*_1 & & & & & & \\ p^*_2 & 0 & 0 & q^*_2 & & & & \\ & & p^*_3 & 0 & 0 & q^*_3 & & \\ & & & \ddots & \ddots & \ddots & \ddots & \\ & & & & & p^*_{S-1} & 0 & 0 & q^*_{S-1} \\ & & & & & & p^*_S & 0. \end{pmatrix} \tag{3.30}$$

The matrix elements of $\mathbf{G}^*_S$ are given by

$$\begin{aligned} p^*_j &= \frac{\sinh((\beta_j - m_j)v)}{\sinh((\beta_j - \alpha_j)v)}, \qquad \text{for } j = 2, \dots, S, \\ q^*_j &= \frac{\sinh((m_j - \alpha_j)v)}{\sinh((\beta_j - \alpha_j)v)}, \qquad \text{for } j = 1, \dots, S-1. \end{aligned} \tag{3.31}$$

Proof. On Ω_1, using (3.14) the Laplace transform of the error, $\widehat{e}^k_{1,m_1}(s)$, can be written as

$$\widehat{e}^k_{1,m_1}(s) = \frac{\sinh\left((m_1 - \alpha_1)v\right)}{\sinh\left((\beta_1 - \alpha_1)v\right)} \widehat{e}^{k-1}_{2,\beta_1}(s) = q^*_1 \widehat{e}^{k-1}_{2,\beta_1}(s), \tag{3.32}$$

where q^*_1 is defined in (3.31).

On Ω_j, for $j = 2, \dots, S-1$, using (3.14), the Laplace transform of the error, $\widehat{e}^k_{j,m_j}(s)$, for $j = 2, \dots, S-1$, can be written as

$$\begin{aligned} \widehat{e}^k_{j,m_j}(s) &= \frac{\sinh((\beta_j - m_j)v)}{\sinh((\beta_j - \alpha_j)v)} \widehat{e}^{k-1}_{j-1,\alpha_j}(s) + \frac{\sinh((m_j - \alpha_j)v)}{\sinh((\beta_j - \alpha_j)v)} \widehat{e}^{k-1}_{j+1,\beta_j}(s) \\ &= p^*_j \widehat{e}^{k-1}_{j-1,\alpha_j}(s) + q^*_j \widehat{e}^{k-1}_{j+1,\beta_j}(s), \end{aligned} \tag{3.33}$$

where p^*_j and q^*_j are defined in (3.31).

Finally, on Ω_S, using (3.14), the Laplace transform of the error, $\widehat{e}^k_{S,m_S}(s)$, can be written as

$$\widehat{e}^k_{S,m_S}(s) = \frac{\sinh((\beta_S - m_S)v)}{\sinh((\beta_S - \alpha_S)v)} \widehat{e}^{k-1}_{S-S,\alpha_S}(s) = p^*_S \widehat{e}^{k-1}_{S-1,\alpha_S}(s), \tag{3.34}$$

where p_S is defined in (3.31).

Writing (3.32), (3.34), and (3.33) in matrix form we arrive at (3.29). ∎

We are now in a position to prove convergence of the SWR algorithm at all mesh points.

Theorem 3.11. *Suppose $\theta \in [\frac{1}{2}, 1]$. If $\lambda_+ = e^v$, then the maximum error for the fully discrete multi-domain SWR iteration (3.8) occurs on the boundaries x_{β_j}, for $j = 1, \ldots, S-1$, and x_{α_j}, for $j = 2, \ldots, S$. The Laplace transform of the errors satisfy*

$$\left\|\zeta^k\right\|_\infty \leq \left\|\xi^{k-1}\right\|_\infty, \tag{3.35}$$

where ζ^k and ξ^k are defined in (3.28) and (3.19), and hence the algorithm converges at each grid node.

Proof. The result follows by showing $\|\mathbf{G}_S^*\|_\infty = 1$, where $\mathbf{G}_S^*$ is defined in (3.30). The infinity norm of $\mathbf{G}_S^*$ is

$$\|\mathbf{G}_S^*\|_\infty = \max\left\{|q_1^*|, |p_S^*|, \max_{j=2,\ldots,S-1}\left\{|p_j^*| + |q_j^*|\right\}\right\}, \tag{3.36}$$

where p_j^* and q_j^* are defined in (3.31).

Using Lemma 2.12, for $s \in R_s$, we have

$$\begin{aligned}
|q_1^*| &= \left|\frac{\sinh((m_1-\alpha_1)v)}{\sinh((\beta_1-\alpha_1)v)}\right| \leq 1, && \text{for } m_1 = \alpha_1, \ldots, \beta_1,\\
|p_S^*| &= \left|\frac{\sinh((\beta_S-m_S)v)}{\sinh((\beta_S-\alpha_S)v)}\right| \leq 1, && \text{for } m_S = \alpha_S, \ldots, \beta_S,\\
|p_j^*| + |q_j^*| &= \left|\frac{\sinh((\beta_j-m_j)v)}{\sinh((\beta_j-\alpha_j)v)}\right| + \left|\frac{\sinh((m_j-\alpha_j)v)}{\sinh((\beta_j-\alpha_j)v)}\right| \leq 1, && \text{for } m_j = \alpha_j, \ldots, \beta_j.
\end{aligned} \tag{3.37}$$

From (3.37), we have $\|\mathbf{G}_S^*\|_\infty = 1$, and the inequality (3.35) follows. The convergence at the interior nodes follows from inequality (3.35) and the convergence at the interfaces obtained in Lemma 3.9. □

Although the theorem above guarantees the convergence in the frequency domain (at all nodes), it does not provide a convergence rate (due to the generality of the domain splitting). The convergence in the time domain does follow, however, from the definition of the discrete Laplace transform.

In general, the contraction matrix $\mathbf{G}_S$ is not symmetric, nor Toeplitz, for all l_j and δ_j. This makes it difficult to find a closed-form upper bound for its norm. To find such upper bound the next Corollary considers a special form of $\mathbf{G}_S$, resulting from the restriction to a uniform partitioning with equal sized overlaps and subdomain sizes.

Corollary 3.12. *Suppose $\theta \in [\frac{1}{2}, 1]$ and the spatial domain has been partitioned into S equal sized overlapping subdomains of width $l\Delta x$ with equal overlap $\delta\Delta x$, with $l = (2N-\delta)/S+\delta$. If $\lambda_+ = e^v$ then the Laplace transforms of the errors in the approximation generated by the fully discrete multi-subdomain SWR iteration (3.8) at the interfaces x_{β_j}, for $j = 1, \ldots, S-1$, and x_{α_j}, for $j = 2, \ldots, S$, satisfy*

$$\xi^k = \mathbf{M}_S \xi^{k-1}, \tag{3.38}$$

where ξ^k is defined in (3.19) and $\mathbf{M}_S \in \mathbb{C}^{2(S-1)\times 2(S-1)}$ is given by

$$\mathbf{M}_S = \begin{pmatrix}
0 & r & & & & & & & & \\
r & 0 & 0 & q & & & & & & \\
q & 0 & 0 & r & & & & & & \\
 & & r & 0 & 0 & q & & & & \\
 & & q & 0 & 0 & r & & & & \\
 & & & \ddots & \ddots & \ddots & \ddots & \ddots & & \\
 & & & & & & r & 0 & 0 & q \\
 & & & & & & q & 0 & 0 & r \\
 & & & & & & & & r & 0
\end{pmatrix}. \tag{3.39}$$

The matrix elements are given by

$$r = \frac{\sinh((l-\delta)v)}{\sinh(lv)}, \quad \text{and} \quad q = \frac{\sinh(\delta v)}{\sinh(lv)}. \tag{3.40}$$

We now proceed to analyze the two norm of the contraction matrix $\mathbf{M}_S$. For the following analysis, we assume that S is odd. The case where S is even can be dealt with in a similar way with small modifications.

Lemma 3.13. *Suppose that S is odd and the spatial domain has been partitioned into S equal sized overlapping subdomains of width $l\Delta x$ and with equal overlap $\delta\Delta x$, with $l = (2N-\delta)/S + \delta$. If $\lambda_+ = e^v$, then the Laplace transforms of the errors in the approximation generated by the multi-domain fully discrete SWR iteration (3.8) at the interfaces x_{β_j}, for $j = 1, \ldots, S-1$, and x_{α_j}, for $j = 2, \ldots, S$, satisfy*

$$\tilde{\xi}^k = \tilde{\mathbf{M}}_S \tilde{\xi}^{k-1}, \tag{3.41}$$

where

$$\tilde{\xi}^k = \begin{pmatrix} \xi_o^k \\ \xi_e^k \end{pmatrix} \quad \text{and} \quad \tilde{\mathbf{M}}_S = \left(\begin{array}{c|c} & \mathbf{\Phi}_S \\ \hline \mathbf{\Psi}_S & \end{array}\right). \tag{3.42}$$

Here,

$$\begin{aligned} \xi_o^k &= \left(\widehat{e}_{1,\alpha_2}^k(s), \widehat{e}_{3,\beta_2}^k(s), \widehat{e}_{3,\alpha_4}^k(s), \ldots, \widehat{e}_{S-2,\beta_{S-3}}^k(s), \widehat{e}_{S-2,\alpha_S-1}^k(s), \widehat{e}_{S,\beta_S-1}^k(s)\right)^T, \\ \xi_e^k &= \left(\widehat{e}_{2,\beta_1}^k(s), \widehat{e}_{2,\alpha_3}^k(s), \widehat{e}_{4,\beta_3}^k(s), \widehat{e}_{4,\alpha_5}^k(s), \ldots, \widehat{e}_{S-1,\beta_{S-2}}^k(s), \widehat{e}_{S-1,\alpha_S}^k(s), \right)^T, \end{aligned} \tag{3.43}$$

and $\mathbf{\Phi}_S, \mathbf{\Psi}_S \in \mathbb{C}^{(S-1)\times(S-1)}$ are given by

$$\mathbf{\Phi}_S = \begin{pmatrix} r & & & & & & \\ & r & q & & & & \\ & q & r & & & & \\ & & \ddots & \ddots & & & \\ & & & \ddots & \ddots & & \\ & & & & & r & q \\ & & & & & q & r \\ & & & & & & r \end{pmatrix} \mathbf{\Psi}_S = \begin{pmatrix} r & q & & & & & \\ q & r & & & & & \\ & & \ddots & \ddots & & & \\ & & & \ddots & \ddots & & \\ & & & & & r & q \\ & & & & & q & r \end{pmatrix}, \tag{3.44}$$

where r and q are given by

$$r = \frac{\sinh((l-\delta)v)}{\sinh(lv)}, \quad \text{and} \quad q = \frac{\sinh(\delta v)}{\sinh(lv)}. \tag{3.45}$$

Proof. First, we define the following permutation matrix

$$\mathbf{P}_S = \left(\frac{\mathbf{P}_o}{\mathbf{P}_e}\right), \tag{3.46}$$

where $\mathbf{P}_o, \mathbf{P}_e \in \mathbb{R}^{(S-1)\times 2(S-1)}$ are given by

$$\mathbf{P}_o = \begin{pmatrix} 1 & & & & & & & & \\ & 0 & 0 & 1 & 0 & & & & \\ & 0 & 0 & 0 & 1 & & & & \\ & & & \ddots & \ddots & \ddots & \ddots & & \\ & & & \ddots & \ddots & \ddots & \ddots & & \\ & & & & & & & 0\,0\,1\,0 & \\ & & & & & & & 0\,0\,0\,1 & \\ & & & & & & & & 0\,0\,1 \end{pmatrix} \tag{3.47}$$

and

$$\mathbf{P}_e = \begin{pmatrix} 0\,1\,0 & & & & & & & \\ 0\,0\,1 & & & & & & & \\ & 0\,0\;1\;\;0 & & & & & & \\ & 0\,0\;\;0\;\;1 & & & & & & \\ & & \ddots\;\ddots\;\ddots\;\ddots & & & & \\ & & & & 0\;\;0\;1\,0 & & \\ & & & & 0\;\;0\;\;0\,1 & & \\ & & & & & 0\,0\,1\,0\,0 & \\ & & & & & 0\,0\,0\,1\,0 \end{pmatrix}. \tag{3.48}$$

Multiplying both sides of (3.38) by the permutation matrix $\mathbf{P}_S$, we have

$$\mathbf{P}_S\xi^k = \mathbf{P}_S\mathbf{M}_S\xi^{k-1}. \tag{3.49}$$

The permutation matrix, $\mathbf{P}_S$, is an orthogonal matrix. Using the fact $\mathbf{P}_S^T\mathbf{P}_S = I$, (3.49) can be written as

$$\mathbf{P}_S\xi^k = \mathbf{P}_S\mathbf{M}_S\mathbf{P}_S^T\mathbf{P}_S\xi^{k-1}. \tag{3.50}$$

Letting $\tilde{\xi}^k = \mathbf{P}_S\xi^k$ and $\tilde{\mathbf{M}}_S = \mathbf{P}_S\mathbf{M}_S\mathbf{P}_S^T$, the result follows. □

The next lemma obtains an explicit contraction rate in the two norm for the error at the interfaces for the multidomain fully discrete SWR algorithm.

Lemma 3.14. *Suppose $\theta \in [\frac{1}{2}, 1]$, S is odd and the spatial domain has been partitioned into S equal sized overlapping subdomains of width $l\Delta x$ and with equal overlap $\delta\Delta x$, with $l = (2N-\delta)/S + \delta$. If $\lambda_+ = e^v$, then the two norm of the Laplace transforms of the errors on the interfaces x_{β_j}, for $j = 1, \ldots, S-1$, and x_{α_j}, for $j = 2, \ldots, S$, for the fully discrete SWR iteration, (3.8), converge according to*

$$\left\|\tilde{\xi}^k\right\|_2 \leq \left(1 - 4\frac{\delta(l-\delta)}{l^2}\sin^2\left(\frac{\pi}{2S}\right)\right)\left\|\tilde{\xi}^{k-2}\right\|_2, \tag{3.51}$$

where $\tilde{\xi}^k$ and $\tilde{\mathbf{M}}_S$ are defined in (3.42).

Proof. Using (3.42) the square of $\tilde{\mathbf{M}}_S$ is

$$\tilde{\mathbf{M}}_S^2 = \left(\begin{array}{c|c} \boldsymbol{\Phi}_S\boldsymbol{\Psi}_S & \\ \hline & \boldsymbol{\Psi}_S\boldsymbol{\Phi}_S \end{array}\right), \tag{3.52}$$

where $\boldsymbol{\Phi}_S\boldsymbol{\Psi}_S, \boldsymbol{\Psi}_S\boldsymbol{\Phi}_S \in \mathbb{C}^{(S-1)\times(S-1)}$ are given by

$$\boldsymbol{\Phi}_S\boldsymbol{\Psi}_S = \begin{pmatrix} r^2 & rq & & & & \\ rq & r^2 & rq & q^2 & & \\ q^2 & rq & r^2 & rq & & \\ & \ddots & \ddots & \ddots & \ddots & \\ & & & rq & r^2 & rq\;\;q^2 \\ & & & q^2 & rq & r^2\;\;rq \\ & & & & & rq\;\;r^2 \end{pmatrix} \tag{3.53}$$

and

$$\mathbf{\Psi}_S\mathbf{\Phi}_S = \begin{pmatrix} r^2 & rq & q^2 & & & & & \\ rq & r^2 & rq & & & & & \\ & rq & r^2 & rq & q^2 & & & \\ & q^2 & rq & r^2 & rq & & & \\ & & \ddots & \ddots & \ddots & \ddots & & \\ & & & & rq & r^2 & rq & q^2 \\ & & & & q^2 & rq & r^2 & rq \\ & & & & & rq & r^2 & rq \\ & & & & & q^2 & rq & r^2 \end{pmatrix}. \tag{3.54}$$

Since $\tilde{\mathbf{M}}_S^2$ is a block diagonal matrix, we have

$$\left\|\tilde{\mathbf{M}}_S^2\right\|_2 = \max\{\|\mathbf{\Phi}_S\mathbf{\Psi}_S\|_2, \|\mathbf{\Psi}_S\mathbf{\Phi}_S\|_2\}. \tag{3.55}$$

To find an upper bound for $\|\mathbf{\Phi}_S\mathbf{\Psi}_S\|_2$ and $\|\mathbf{\Psi}_S\mathbf{\Phi}_S\|_2$, we follow the same procedure as in [9]. We rewrite the matrices $\mathbf{\Phi_S}$ and $\mathbf{\Psi_S}$ as

$$\begin{aligned} \mathbf{\Phi}_S\mathbf{\Psi}_S &= \mathbf{T}_S + q^2\mathbf{F}_1, \\ \mathbf{\Psi}_S\mathbf{\Phi}_S &= \mathbf{T}_S + q^2\mathbf{F}_2, \end{aligned} \tag{3.56}$$

where $\mathbf{T}_S = \text{tridiag}(rq, r^2, rq)$, $q^2\mathbf{F}_1 = \mathbf{\Phi}_S\mathbf{\Psi}_S - \mathbf{T}_S$, and $q^2\mathbf{F}_2 = \mathbf{\Psi}_S\mathbf{\Phi}_S - \mathbf{T}_S$.

Applying the two norm on both sides of (3.56) and using the triangle inequality, we have

$$\begin{aligned} \|\mathbf{\Phi}_S\mathbf{\Psi}_S\|_2 &\le \|\mathbf{T}_S\|_2 + |q|^2\|\mathbf{F}_1\|_2, \\ \|\mathbf{\Psi}_S\mathbf{\Phi}_S\|_2 &\le \|\mathbf{T}_S\|_2 + |q|^2\|\mathbf{F}_2\|_2. \end{aligned} \tag{3.57}$$

The matrices, $\mathbf{F}_j$, for $j = 1, 2$, have only $O(S-1)$ entries, which are all ones. The structure of the $\mathbf{F}_j$ for $j = 1, 2$ then implies $\|\mathbf{F}_j\|_2 = 1$, for $j = 1, 2$.

The complex tridiagonal matrix, $\mathbf{T}_S$, is normal, $\mathbf{T}_S^H\mathbf{T}_S = \mathbf{T}_S\mathbf{T}_S^H$ (where $\mathbf{T}_S^H$ is the conjugate transpose of $\mathbf{T}_S$), this implies that

$$\|\mathbf{T}_S\|_2 = \rho(\mathbf{T}_S), \tag{3.58}$$

where $\rho(\mathbf{T}_S)$ is the spectral radius of $\mathbf{T}_S$.

It is well-known, see *e.g.* [21, 22], that the eigenvalues of $\mathbf{T}_S$, are given by

$$\mathbf{eig}_\ell(\mathbf{T_S}) = r^2 + 2\sqrt{r^2q^2}\cos\left(\frac{\ell\pi}{S}\right) = r^2 + 2\sqrt{|r|^2|q|^2}e^{i(\arg(r)+\arg(q))/2}\cos\left(\frac{\ell\pi}{S}\right), \tag{3.59}$$

for $\ell = 1, \ldots, S-1$, where $\arg(r)$ is the complex argument of r.

The spectral radius of $\mathbf{T}_S$ can be bounded as

$$\|\mathbf{T}_S\|_2 = \rho(\mathbf{T}_S) \le |r|^2 + 2|r||q|\cos\left(\frac{\pi}{S}\right). \tag{3.60}$$

Using (3.60), (3.57) and the fact that $\|\mathbf{F}_j\|_2 = 1$, for $j = 1, 2$, then the spectral radius of $\tilde{\mathbf{M}}_S^2$ can then be bounded as

$$\left\|\tilde{\mathbf{M}}_S^2\right\|_2 \le |r|^2 + |q|^2 + 2|r||q|\cos\left(\frac{\pi}{S}\right). \tag{3.61}$$

Using (3.61) and the supremum property, the error recursion formula, (3.51), follows.

Now, to prove the convergence, we use the fact that, for any finite $S \geq 1$ $0 < \cos\left(\frac{\pi}{S}\right) < 1$, the trigonometric identity $\cos\left(\frac{\pi}{S}\right) = 1 - 2\sin^2\left(\frac{\pi}{2S}\right)$, (3.45), (2.21) and supremum property. Then (3.61) can be written and bounded as

$$\begin{aligned}\left\|\tilde{\mathbf{M}}_S^2\right\|_2 \leq \left(|r|^2 + |q|^2 + 2|r||q|\cos\left(\frac{\pi}{S}\right)\right) &< \frac{(l-\delta)^2 + \delta^2 + 2(l-\delta)\delta\left(1 - 2\sin^2\left(\frac{\pi}{2S}\right)\right)}{l^2} \\ &= 1 - 4\frac{\delta(l-\delta)}{l^2}\sin^2\left(\frac{\pi}{2S}\right).\end{aligned} \tag{3.62}$$

Clearly for $0 < \delta < l$ we have $\left(1 - 4\frac{\delta(l-\delta)}{l^2}\sin^2\left(\frac{\pi}{2S}\right)\right) < 1$, and the convergence follows. □

The following lemma is used to prove that a maximum principle holds in the two norm in the multi-domain case. We begin with a representation of the error at an arbitrary node and then provide norms of the coefficient matrix.

Lemma 3.15. *Suppose $\theta \in [\frac{1}{2}, 1]$, S is odd and the spatial domain has been partitioned into S equal sized overlapping subdomains of width $l\Delta x$ and with equal overlap $\delta\Delta x$, with $l = (2N-\delta)/S + \delta$. If $\lambda_+ = e^v$, then the Laplace transforms of the errors, ζ^k, in the approximation generated by the multi-domain fully discrete SWR iteration (3.8) and the Laplace transforms of the errors at the interfaces, ξ^k, satisfy*

$$\zeta^k = \mathbf{M}_S^* \xi^{k-1}, \tag{3.63}$$

where ζ^k is defined in (3.28), ξ^k is defined in (3.19) and $\mathbf{M}_S^* \in \mathbb{C}^{S\times 2(S-1)}$ is given by

$$\mathbf{M}_S^* = \begin{pmatrix} 0 & \widehat{q}_1^* & & & & & & \\ \widehat{p}_2^* & 0 & 0 & \widehat{q}_2^* & & & & \\ & \widehat{p}_3^* & 0 & 0 & \widehat{q}_3^* & & & \\ & & \ddots & \ddots & \ddots & \ddots & & \\ & & & & \widehat{p}_{S-1}^* & 0 & 0 & \widehat{q}_{S-1}^* \\ & & & & & & \widehat{p}_S^* & 0 \end{pmatrix}. \tag{3.64}$$

Here, $m_j \in \{\alpha_j, \ldots, \beta_j\}$, for $j = 1, \ldots, S$, and

$$\begin{aligned} \widehat{p}_j^* &= \frac{\sinh((\beta_j - m_j)v)}{\sinh(lv)}, \qquad \text{for } j = 2, \ldots, S, \\ \widehat{q}_j^* &= \frac{\sinh((m_j - \alpha_j)v)}{\sinh(lv)}, \qquad \text{for } j = 1, \ldots, S-1. \end{aligned} \tag{3.65}$$

Moreover,

$$\|\mathbf{M}_S^*\|_p = 1, \quad \text{for} \quad p = 1, \infty. \tag{3.66}$$

Proof. The representation of the Laplace transforms of the errors at the interior nodes follows from Lemma 3.10 and using the fact that $\beta_j - \alpha_j = l$, for $j = 1, \ldots, S$.

The one and infinity norm of $\mathbf{M}_S^*$ are

$$\begin{aligned} \|\mathbf{M}_S^*\|_1 &= \max_{j=1,\ldots,S}\left\{\left|\widehat{q}_j^*\right|, \left|\widehat{p}_j^*\right|\right\}, \\ \|\mathbf{M}_S^*\|_\infty &= \max\left\{\left|\widehat{q}_1^*\right|, \left|\widehat{p}_S^*\right|, \max_{j=2,\ldots,S-1}\left\{\left|\widehat{p}_j^*\right| + \left|\widehat{q}_j^*\right|\right\}\right\}, \end{aligned} \tag{3.67}$$

where $\widehat{p}_j^*$ and $\widehat{q}_j^*$ are defined in (3.65). Using (2.21) and following the steps in (3.37), the result follows. □

The following lemma shows the relation between the Laplace transforms of the errors at the interior nodes ζ and the permuted Laplace transforms of the errors at the interfaces, $\tilde{\xi}$.

Lemma 3.16. *Suppose that S is odd and the spatial domain has been partitioned into S equal sized overlapping subdomains of width $l\Delta x$ and with equal overlap $\delta\Delta x$, with $l = (2N-\delta)/S + \delta$. If $\lambda_+ = e^v$, then the Laplace transforms of the errors, ζ^k, in the approximation generated by the fully discrete multi-domain SWR iteration, (3.8), and the Laplace transforms of the errors at the interfaces, $\tilde{\xi}^k$, satisfy*

$$\zeta^k = \tilde{\mathbf{M}}_S^* \tilde{\xi}^{k-1}, \tag{3.68}$$

where

$$\tilde{\mathbf{M}}_S^* = \mathbf{M}_S^* \mathbf{P}_S^T. \tag{3.69}$$

Here, $\tilde{\xi}^{k-1}$, $\mathbf{M}_S^*$, and $\mathbf{P}_S^T$ are defined in (3.42), (3.43), (3.64), and (3.46), respectively.

Proof. Using the fact that the permutation matrix, $\mathbf{P}_S$, is an orthogonal matrix, (3.63) can be written as

$$\zeta^k = \mathbf{M}_S^* \mathbf{P}_S^T \mathbf{P}_S \xi^{k-1}. \tag{3.70}$$

using the substitution $\tilde{\mathbf{M}}_S^* = \mathbf{M}_S^* \mathbf{P}_S^T$ and $\tilde{\xi}^{k-1} = \mathbf{P}_S \xi^{k-1}$, we arrive at the required result. □

We now arrive at a discrete maximum principle for the Laplace transforms of the errors in the two norm.

Lemma 3.17. *Suppose $\theta \in [\frac{1}{2}, 1]$ and the spatial domain has been partitioned into S equal sized overlapping subdomains (where S is odd) of width $l\Delta x$ and with equal overlap $\delta\Delta x$, with $l = (2N-\delta)/S + \delta$. If $\lambda_+ = e^v$, then the maximum Laplace transform of the errors in the two norm for the fully discrete SWR iteration, (3.8), occurs on the boundaries. The Laplace transforms of the errors satisfy*

$$\left\|\zeta^k\right\|_2 \le \left\|\tilde{\xi}^{k-1}\right\|_2, \tag{3.71}$$

where ζ^k, $\tilde{\xi}^{k-1}$, $\mathbf{M}_S^*$, and $\mathbf{P}_S^T$ are defined in (3.28), (3.43), (3.42), (3.64), and (3.46), respectively. On the initial line and on the exterior boundaries the error vanishes.

Proof. Applying the two norm on both sides of (3.68)

$$\left\|\zeta^k\right\|_2 \le \left\|\tilde{\mathbf{M}}_S^*\right\|_2 \left\|\tilde{\xi}^{k-1}\right\|_2. \tag{3.72}$$

Using the Riesz–Thorin inequality [20], we have

$$\left\|\tilde{\mathbf{M}}_S^*\right\|_2 \le \sqrt{\left\|\tilde{\mathbf{M}}_S^*\right\|_1 \left\|\tilde{\mathbf{M}}_S^*\right\|_\infty}. \tag{3.73}$$

From the definition of $\tilde{\mathbf{M}}_S^*$ in (3.69) and using (3.66), we have

$$\left\|\tilde{\mathbf{M}}_S^*\right\|_p = \left\|\mathbf{M}_S^* \mathbf{P}_S^T\right\|_p \le \left\|\mathbf{M}_S^*\right\|_p \left\|\mathbf{P}_S^T\right\|_p = 1, \quad \text{for} \quad p = 1, \infty. \tag{3.74}$$

From (3.74) the result follows. □

Now we arrive at the point where we can prove the convergence and obtain an explicit contraction in the two norm.

Theorem 3.18. *Suppose $\theta \in [\frac{1}{2}, 1]$, S is odd and the spatial domain has been partitioned into S equal sized overlapping subdomains of width $l\Delta x$ and with equal overlap $\delta\Delta x$, with $l = (2N-\delta)/S + \delta$. If $\lambda_+ = e^v$, then the fully discrete multi-domain SWR iteration (3.8) for the heat equation converges at the linear rate in the two norm. The Laplace transforms of the errors satisfy*

$$\left\|\zeta^{2k+1}\right\|_2 \le \left(1 - 4\frac{\delta(l-\delta)}{l^2}\sin^2\left(\frac{\pi}{2S}\right)\right)^k \left\|\tilde{\xi}^0\right\|_2, \tag{3.75}$$

where ζ^k and $\tilde{\xi}^k$ are defined in (3.28), (3.42), and (3.43), respectively.

Proof. The result follows from Lemma 3.14 and induction. In fact

$$\left\|\zeta^{2k+1}\right\|_2 = \left\|\tilde{M}_S^*\tilde{\xi}^{2k}\right\|_2 \leq \left\|\tilde{M}_S^*\right\|_2 \left\|\tilde{\xi}^{2k}\right\|_2 \leq \left(|r|^2 + |q|^2 + 2|r||q|\cos\left(\frac{\pi}{S}\right)\right)^k \left\|\tilde{\xi}^0\right\|_2.$$

Again for $0 < \delta < l$ we have $\left(|r|^2 + |q|^2 + 2|r||q|\cos\left(\frac{\pi}{S}\right)\right) \leq \left(1 - 4\frac{\delta(l-\delta)}{l^2}\sin^2\left(\frac{\pi}{2S}\right)\right) < 1$, and the convergence follows from (3.62). □

The following corollary shows the two norm convergence at the interfaces in the time domain $t > 0$.

Corollary 3.19. *Suppose $\theta \in [\frac{1}{2}, 1]$ and the spatial domain has been partitioned into S equal sized overlapping subdomains (S is odd) of width $l\Delta x$ with equal overlap $\delta\Delta x$, with $l = (2N - \delta)/S + \delta$. If $\lambda_+ = e^v$ then the two norm of the errors in the approximation generated by the fully discrete multi-subdomain SWR iteration (3.8) in the time domain at the interfaces x_{β_j}, for $j = 1, \ldots, S-1$, and x_{α_j}, for $j = 2, \ldots, S$, for $t > 0$ satisfy*

$$\left\|\chi^k\right\|_2 \leq \left(1 - 4\frac{\delta(l-\delta)}{l^2}\sin^2\left(\frac{\pi}{2S}\right)\right)\left\|\chi^{k-2}\right\|_2, \tag{3.76}$$

where χ^k is given by

$$\chi^k = \left(\left\|\mathbf{e}^k_{1,\alpha_2}\right\|_2, \left\|\mathbf{e}^k_{2,\beta_1}\right\|_2, \ldots, \left\|\mathbf{e}^k_{S-1,\alpha_S}\right\|_2, \left\|\mathbf{e}^k_{S,\beta_S-1}\right\|_2\right)^T. \tag{3.77}$$

Here, $\|\mathbf{e}^k_{j,\alpha_{j+1}}\|_2^2 = \sum_{n=0}^{\infty}\left|e^k_{j,\alpha_{j+1}}(n)\right|^2$, for $j = 1, \ldots, S-1$, and $\|\mathbf{e}^k_{j,\beta_{j-1}}\|_2^2 = \sum_{n=0}^{\infty}\left|e^k_{j,\beta_{j-1}}(n)\right|^2$, for $j = 2, \ldots, S$.

Proof. The proof of Corollary 3.19 follows from Lemma 3.14 and Parseval's identity (2.35). □

The convergence in the time domain at all the interior nodes follows from convergence at the interfaces, x_{β_j}, for $j = 1, \ldots, S-1$, and x_{α_j}, for $j = 2, \ldots, S$, for $t > 0$, Corollary 3.19, and the discrete maximum principle in the time domain.

Like the two subdomain case, in practice, we integrate in time using θ-method over a bounded time interval $(0, T]$. This allow exchanging the information between the subdomains at the end of the time interval T. This convergence result is given next.

Corollary 3.20. *Suppose $\theta \in [\frac{1}{2}, 1]$ and the spatial domain has been partitioned into S equal sized overlapping subdomains (S is odd) of width $l\Delta x$ with equal overlap $\delta\Delta x$, with $l = (2N - \delta)/S + \delta$. If $\lambda_+ = e^v$ then the two norm of the errors in the approximation generated by the fully discrete multi-subdomain SWR iteration (3.8) in the time domain at the interfaces x_{β_j}, for $j = 1, \ldots, S-1$, and x_{α_j}, for $j = 2, \ldots, S$, for $t \in (0, T]$, satisfy*

$$\left\|\tilde{\chi}^k\right\|_2 \leq \sup_{\tilde{R}_s}\left(|r|^2 + |q|^2 + 2|r||q|\cos\left(\frac{\pi}{S}\right)\right)\left\|\tilde{\chi}^{k-2}\right\|_2, \tag{3.78}$$

where $\tilde{\chi}^k$ is

$$\tilde{\chi}^k = \left(\left\|\tilde{\mathbf{e}}^k_{1,\alpha_2}\right\|_2, \left\|\tilde{\mathbf{e}}^k_{2,\beta_1}\right\|_2, \ldots, \left\|\tilde{\mathbf{e}}^k_{S-1,\alpha_S}\right\|_2, \left\|\tilde{\mathbf{e}}^k_{S,\beta_S-1}\right\|_2\right)^T. \tag{3.79}$$

Here, $\|\tilde{\mathbf{e}}^k_{j,\alpha_{j+1}}\|_2^2 = \sum_{n=0}^{T/\Delta t}\left|e^k_{j,\alpha_{j+1}}(n)\right|^2$, for $j = 1, \ldots, S-1$, and $\|\tilde{\mathbf{e}}^k_{j,\beta_{j-1}}\|_2^2 = \sum_{n=0}^{T/\Delta t}\left|e^k_{j,\beta_{j-1}}(n)\right|^2$, for $j = 2, \ldots, S$. Here, we assume that $T/\Delta t$ is an integer.

Proof. The proof of Corollary 3.20 follows from restricting the frequencies considered in Lemma 3.14 to $\pi/T \leq |\omega| \leq \pi/\Delta t$ and using Parseval's identity (2.36). □

We will use the result of Corollary 3.20 to numerically illustrate the convergence at the interfaces in the time domain for multi-domain case in Section 4.

4. Numerical results

In this section, we demonstrate the numerical convergence of the classical SWR algorithm for the following heat equation

$$\begin{aligned} u_t &= u_{xx} - e^{-(t-1)^2-\left(x-\frac{1}{4}\right)^2}, && -1 < x < 1,\ 0 < t < 1, \\ u(x,0) &= 1, && -1 < x < 1, \\ u(-1,t) &= 2e^{-2t} - e^{-t}, && 0 < t < 1, \\ u(1,t) &= e^{-t}, && 0 < t < 1. \end{aligned} \tag{4.1}$$

The above example has been considered in [9] with $0 < x < 1$ and $0 < t < 3$.

For all the numerical experiments we discretize the spatial and temporal domains with $\Delta x = \Delta t = 0.01$. We use the initial condition to generate a constant-in-time initial guess for the SWR algorithm at the interior (artificial) interfaces.

First we solve the heat equation (4.1) on two subdomains with different overlaps: $\delta = 10,\ 20$ and 30. For these three cases, we consider the subdomains $\Omega_1^{0.01} = \{-1, \ldots, x_\beta\}$ and $\Omega_2^{0.01} = \{x_\alpha, \ldots, 1\}$ where

$$(x_\alpha, x_\beta) \in \{(-0.05, 0.05), (-0.1, 0.1), (-0.15, 0.15)\}.$$

Figure 6 shows the error between the single domain solution and the subdomain solutions generated by the SWR algorithm at x_β for $\theta = 1/2$ (*left*) and $\theta = 1$ (*right*). The solid black lines show the actual discrete errors (for varying overlaps), $\|\tilde{\mathbf{e}}_{2,\beta}^k\|_2$, measured in the two norm in the time domain, as defined in Corollary 2.19. The red and the blue dashed lines are the theoretically predicted errors on bounded (B) and unbounded (UB) time intervals, respectively, at every second iteration, $\left\|\tilde{\mathbf{e}}_{2,\beta}^{2k,B}\right\|_2 = \sup_{\tilde{R}_s}\left|\frac{\sinh((l_1-\delta)v)}{\sinh(l_1 v)}\frac{\sinh((l_2-\delta)v)}{\sinh(l_2 v)}\right|\left\|\tilde{\mathbf{e}}_{2,\beta}^{2(k-1)}\right\|_2$ and $\left\|\tilde{\mathbf{e}}_{2,\beta}^{2k,UB}\right\|_2 = \frac{(l_1-\delta)}{l_1}\frac{(l_2-\delta)}{l_2}\left\|\tilde{\mathbf{e}}_{2,\beta}^{2(k-1)}\right\|_2$, for $k = 1, 2, \ldots$. The supremum of the contraction rate on $\tilde{R}_s$ has been evaluated numerically. As expected from Corollary 2.19, the results show that the predicted error on a bounded time interval is bounded by the predicted error on an unbounded time interval for $\theta = \frac{1}{2}$ and $\theta = 1$. More importantly, the experimental results and the theoretical bounds are quite close.

We note that in the figure we have curves rather than the straight lines that may be expected from the linear convergence result. The curves arise due to the definitions of $\tilde{\mathbf{e}}^{\mathbf{2k,B}}$ and $\tilde{\mathbf{e}}^{\mathbf{2k,UB}}$. In these definitions you can see that we are only comparing the **per-step decrease** in the errors. On the right hand side of the definition for $\tilde{\mathbf{e}}_{2,\beta}^{2k,B}$, for instance, we have $\|\tilde{\mathbf{e}}_{2,\beta}^{2(k-1)}\|_2$, which is the two norm of the actual error in the time domain two steps before.

We now solve problem (4.1)) using SWR with $S = 3, 5$ and 7 subdomains with a fixed overlap size of $\delta = 20$. The solid black line in Figure 7 shows the convergence profile of the two norm of the actual error $\left\|\tilde{\chi}^k\right\|_2$ in the time domain.

The red and the blue dashed lines are again the theoretically predicted errors on the bounded and the unbounded time intervals at every second iteration, defined as

$$\left\|\tilde{\chi}^{2k,B}\right\|_2 = \sup_{\tilde{R}_s}\left(|r|^2 + |q|^2 + 2|r||q|\cos\left(\frac{\pi}{S}\right)\right)\left\|\tilde{\chi}^{2(k-1)}\right\|_2$$

and

$$\left\|\tilde{\chi}^{2k,UB}\right\|_2 = \left(1 - 4\frac{\delta(l-\delta)}{l^2}\sin^2\left(\frac{\pi}{2S}\right)\right)\left\|\tilde{\chi}^{2(k-1)}\right\|_2,$$

for $k = 1, 2, 3, \ldots$.

Again, the supremum of the contraction rate on $\tilde{R}_s$ has been evaluated numerically. The results again show close agreement between the experimental results and the theoretical bounds for both values of θ and the different numbers of subdomains tested.

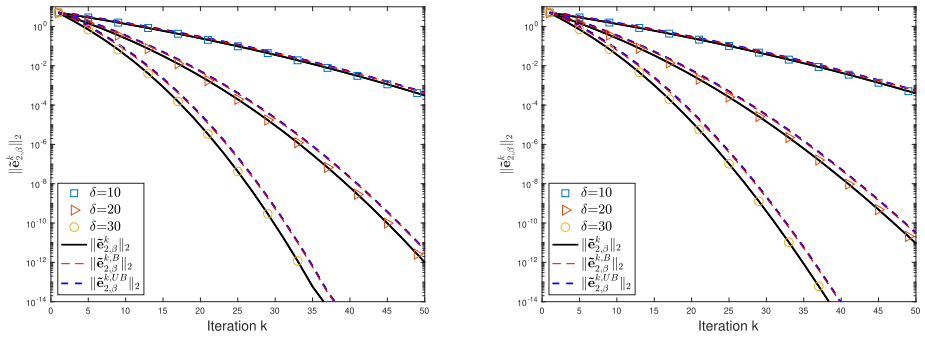

(a) (b)

FIGURE 6. Convergence of the SWR algorithm for (4.1) using the θ-method on two subdomains with $\theta = 1/2$ (*left*) and $\theta = 1$ (*right*). (a) $\theta = 1/2$ and (b) $\theta = 1$.

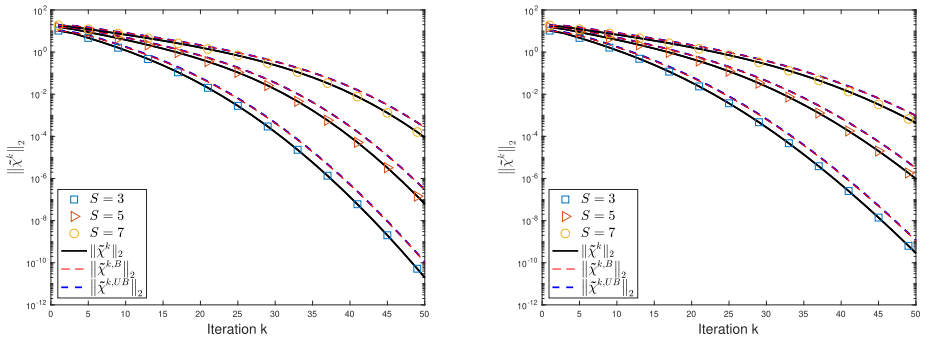

(a) (b)

FIGURE 7. Convergence of the SWR algorithm for (4.1) using the θ-method for different numbers of subdomains for $\theta = 1/2$ (*left*) and $\theta = 1$ (*right*). (a) $\theta = 1/2$ and (b) $\theta = 1$.

5. Conclusion

In this paper, we considered the fully discrete convergence analysis of SWR on a bounded spatial and time domain for the heat equation. Bounding the spatial domain allows a first multi-domain, fully discrete convergence analysis, while bounding the time domain allows us to study the algorithm implemented in practice which exchanges information between neighboring subdomains at the end of the time window T.

We have proved the convergence of the discrete classical SWR- algorithm on a bounded spatial domain using an arbitrary, finite number of subdomains for the heat equation using the θ-method for $\theta \in \left[\frac{1}{2}, 1\right]$ as the time integrator. The imposition of a bounded spatial domain leads to a new, and much more complicated convergence factor to analyze. On an unbounded time interval the discrete classical SWR-algorithm has a robust convergence rate whose upper bound is independent of the choice of the parameters Δx, Δt and θ, for $\theta \in \left[\frac{1}{2}, 1\right]$.

On two subdomains, we prove the convergence of the SWR-algorithm on a bounded spatial domain and on bounded and unbounded time intervals. On a bounded time interval, the contraction rate is bounded by the contraction rate for the unbounded time interval.

For the general multidomain case with non-equal size overlaps or partitioning, we proved the convergence in the frequency space at the interfaces and at all interior nodes. The convergence in the time domain then follows.

Due to the generality of the problem, we were not able to find an explicit form for the contraction rate in the time domain for this case. With equal size overlap and subdomains a convergence result in the frequency space was obtained in the two norm, a time domain result then follows from Parseval's identity. We introduced and proved the maximum principle at the discrete level for the two and multi subdomain cases, and then used it to show convergence at all interior nodes.

The techniques demonstrated above will prove useful to handle the analysis of fully discrete SWR algorithms (on bounded spatial domains) for other classes of linear PDEs and choices of time integrators. It is important to identify any *necessary* conditions required on the time integrator to allow convergence of the discrete SWR algorithm. Our approach provides an initial framework for two-dimensional extensions and for nonlinear problems discretized by linearizing approaches (such as Rosenbrock methods). Work is also underway to use this framework to study the fully discrete optimized Schwarz waveform relaxation algorithm on a finite spatial domain. This algorithm provides a parameter which may be tuned to accelerate the convergence of the algorithm. Dirichlet–Neumann interface conditions may be studied in a similar manner.

Acknowledgements. The authors would like to thank Martin Gander and Felix Kwok for their valuable advice that helped us finish the analysis for this paper.

Conflicts of interest. Not applicable.

Competing interests. Not applicable.

Funding. This research was funded by Dr. Haynes' NSERC Discovery Grant (Canada), RGPIN 2018-04881.

Data availability. The datasets generated during and/or analysed during the current study are available from the authors upon reasonable request.

Code availability. The custom code written during the current study are available from the authors upon reasonable request.

References

[1] M.D. Al-Khaleel, M.J. Gander and A.E. Ruehli, A mathematical analysis of optimized waveform relaxation for a small RC circuit. *Appl. Numer. Math.* **75** (2014) 61–76.

[2] M.D. Al-Khaleel, M.J. Gander and A.E. Ruehli, Optimization of transmission conditions in waveform relaxation techniques for RC circuits. *SIAM J. Numer. Anal.* **52** (2014) 1076–1101.

[3] D. Bennequin, M.J. Gander and L. Halpern, A homographic best approximation problem with application to optimized Schwarz waveform relaxation. *Math. Comput.* **78** (2009) 185–185.

[4] D. Bennequin, M.J. Gander, L. Gouarin and L. Halpern, Optimized Schwarz waveform relaxation for advection reaction diffusion equations in two dimensions. *Numer. Math.* **134** (2016) 513–567.

[5] J.R. Cannon, The one-dimensional heat equation, in *Encyclopedia of Mathematics and its Applications*. Vol. 23. Addison-Wesley Publishing Company, Advanced Book Program, Reading, MA (1984). With a foreword by Felix E. Browder.

[6] S. Clement, F. Lemarié and E. Blayo, Discrete analysis of schwarz waveform relaxation for a diffusion reaction problem with discontinuous coefficients. *SMAI J. Comput. Math.* **8** (2022) 99–124.

[7] M.J. Gander, A waveform relaxation algorithm with overlapping splitting for reaction diffusion equations. *Numer. Linear Algebra Appl.* **6** (1999) 125–145.

[8] M.J. Gander, Optimized Schwarz methods. *SIAM J. Numer. Anal.* **44** (2006) 699–731.

[9] M.J. Gander and A.M. Stuart, Space-time continuous analysis of waveform relaxation for the heat equation. *SIAM J. Sci. Comput.* **19** (1998) 2014–2031.

[10] M.J. Gander and A.E. Ruehli, Optimized waveform relaxation methods for RC type circuits. *IEEE Trans. Circuits Syst. I Regul. Pap.* **51** (2004) 755–768.

[11] M.J. Gander and C. Rohde, Overlapping Schwarz waveform relaxation for convection-dominated nonlinear conservation laws. *SIAM J. Sci. Comput.* **27** (2005) 415–439.

[12] M.J. Gander and L. Halpern, Absorbing boundary conditions for the wave equation and parallel computing. *Math. Comput.* **74** (2005) 153–176.

[13] M.J. Gander and L. Halpern, Optimized Schwarz waveform relaxation methods for advection reaction diffusion problems. *SIAM J. Numer. Anal.* **45** (2007) 666–697.

[14] M.J. Gander, L. Halpern and F. Nataf, Optimal Schwarz waveform relaxation for the one dimensional wave equation. *SIAM J. Numer. Anal.* **41** (2003) 1643–1681.

[15] M.J. Gander, P.M. Kumbhar and A.E. Ruehli, Asymptotic analysis for overlap in waveform relaxation methods for RC type circuits. *J. Sci. Comput.* **84** (2020) 1–24.

[16] E. Giladi and H.B. Keller, Space-time domain decomposition for parabolic problems. *Numer. Math.* **93** (2002) 279–313.
[17] L. Halpern and J. Szeftel, Optimized and quasi-optimal Schwarz waveform relaxation for the one-dimensional Schrödinger equation. *Math. Models Methods Appl. Sci.* **20** (2010) 2167–2199.
[18] R.D. Haynes and K. Mohammad. Fully discrete Schwarz waveform relaxation on two bounded overlapping subdomains, in *Domain Decomposition Methods in Science and Engineering XXV*, Lecture Notes in Computational Science and Engineering. Springer International Publishing, Cham (2020) 159–166.
[19] R.D. Haynes and K. Mohammad, A multirate accelerated Schwarz waveform relaxation method, in *Proceedings of the 26th International Domain Decomposition Methods Conference. Lecture Notes in Computational Science and Engineering*. Springer (2023).
[20] R.A. Horn and C.R. Johnson, *Matrix Analysis*. Second ed. Cambridge University Press, Cambridge (2013).
[21] S. Noschese, L. Pasquini and L. Reichel, Tridiagonal Toeplitz matrices: properties and novel applications. *Numer. Linear Algebra Appl.* **20** (2013) 302–326.
[22] G.D. Smith, Numerical solution of partial differential equations: Finite difference methods, in *Oxford Applied Mathematics and Computing Science Series*. Second ed., The Clarendon Press, Oxford University Press, New York (1978).
[23] J.C. Strikwerda, *Finite Difference Schemes and Partial Differential Equations*, Second ed. Society for Industrial and Applied Mathematics (2004).
[24] S.-L. Wu and M.D. Al-Khaleel, Semi-discrete Schwarz waveform relaxation algorithms for reaction diffusion equations. *BIT* **54** (2014) 831–866.
[25] S.-L. Wu and M.D. Al-Khaleel, Convergence analysis of the Neumann–Neumann waveform relaxation method for time-fractional RC circuits. *Simul. Model. Practice Theory* **64** (2016) 43–56.
[26] S.-L. Wu and M.D. Al-Khaleel, Optimized waveform relaxation methods for RC circuits: discrete case. *ESAIM: Math. Model. Numer. Anal.* **51** (2017) 209–223.
[27] S.-L. Wu and M.D. Al-Khaleel, Parameter optimization in waveform relaxation for fractional-order RC circuits. *IEEE Trans. Circuits Syst. I Regul. Pap.* **64** (2017) 1781–1790.